The ISME Journal, 2024, **18(1)**, wrae160
https://doi.org/10.1093/ismejo/wrae160
Advance access publication: 14 August 2024
Original Article

Nitrite-oxidizing bacteria adapted to low-oxygen conditions dominate nitrite oxidation in marine oxygen minimum zones

Samantha G. Fortin [1,*], Xin Sun [2], Amal Jayakumar [1], Bess B. Ward [1]

[1]Department of Geosciences, Princeton University, Princeton, NJ 08544, United States
[2]Department of Global Ecology, Carnegie Institution for Science, Stanford, CA 94305, United States

*Corresponding author: Samantha G. Fortin, Guyot Hall, Princeton University, Princeton, NJ 08544, United States. Email: sf3033@princeton.edu

Abstract

Nitrite is a central molecule in the nitrogen cycle because nitrite oxidation to nitrate (an aerobic process) retains fixed nitrogen in a system and its reduction to dinitrogen gas (anaerobic) reduces the fixed nitrogen inventory. Despite its acknowledged requirement for oxygen, nitrite oxidation is observed in oxygen-depleted layers of the ocean's oxygen minimum zones (OMZs), challenging the current understanding of OMZ nitrogen cycling. Previous attempts to determine whether nitrite-oxidizing bacteria in the anoxic layer differ from known nitrite oxidizers in the open ocean were limited by cultivation difficulties and sequencing depth. Here, we construct 31 draft genomes of nitrite-oxidizing bacteria from global OMZs. The distribution of nitrite oxidation rates, abundance and expression of nitrite oxidoreductase genes, and relative abundance of nitrite-oxidizing bacterial draft genomes from the same samples all show peaks in the core of the oxygen-depleted zone (ODZ) and are all highly correlated in depth profiles within the major ocean oxygen minimum zones. The ODZ nitrite oxidizers are not found in the Tara Oceans global dataset (the most complete oxic ocean dataset), and the major nitrite oxidizers found in the oxygenated ocean do not occur in ODZ waters. A pangenomic analysis shows the ODZ nitrite oxidizers have distinct gene clusters compared to oxic nitrite oxidizers and are microaerophilic. These findings all indicate the existence of nitrite oxidizers whose niche is oxygen-deficient seawater. Thus, specialist nitrite-oxidizing bacteria are responsible for fixed nitrogen retention in marine oxygen minimum zones, with implications for control of the ocean's fixed nitrogen inventory.

Keywords: nitrite-oxidizing bacteria, oxygen minimum zone, nitrification

Introduction

Nitrite is produced and consumed by microbial processes, including denitrification, nitrate respiration, anammox, and nitrification, which require either presence or absence of oxygen. Oceanic oxygen minimum zones (OMZs) are characterized by a permanent subsurface oxygen-deficient zone (ODZ) and a corresponding secondary nitrite peak. OMZs are important hotspots of nitrogen cycling leading to either the conservation, driven by nitrite oxidation to nitrate, or loss, driven by nitrite reduction to dinitrogen gas during denitrification and anammox, of fixed nitrogen. These two steps are assumed to be independent because nitrite oxidation is understood to be an obligately aerobic process, and denitrification and anammox are anaerobic. Evidence [1–4] that nitrite oxidation can occur in samples collected from oxygen-depleted seawater, i.e. seawater where oxygen is below the detection limit and denitrification and anammox occur, therefore places nitrite firmly at the pivot point—the fate of nitrite determines the rate of fixed nitrogen loss. Because the inventory of fixed nitrogen controls primary production across much of the world's oceans [5], the balance of nitrogen retention and removal in OMZs can have significant impacts on ocean biogeochemistry.

In OMZs, nitrite oxidation rates consistently exceed rates of ammonia oxidation, the first step in nitrification, and highest rates often occur in the absence of detectable oxygen [1–4, 6–11]. Both anammox bacteria and nitrite-oxidizing bacteria (NOB) oxidize nitrite to nitrate using the enzyme nitrite oxidoreductase (NXR) [12, 13]. The depth distribution of measured rates of anammox (i.e. N_2 production from NH_4^+ or NO_2^-) is quite different from the distribution of total nitrite oxidation, and the stoichiometry of anammox means that its associated rates of nitrate production are very low. Therefore, most of the observed nitrite oxidation in OMZs cannot be attributed to anammox [6].

Nitrite oxidation, anammox, and denitrification have all been quantified in isotope tracer experiments using natural seawater samples in the same incubation bottles [4, 14], challenging the previous view of the spatial separation of N retention and loss steps. Nitrite oxidation and nitrate reduction rates in oxygen-depleted waters are highly correlated, suggesting an additional nitrogen loop centered in oxygen-depleted waters [4, 15], in which nitrite is rapidly recycled to nitrate at much greater rates than net reduction to dinitrogen gas by anammox or denitrification. Natural abundance isotope data and modeling [16, 17] argue that observed natural abundance isotopic composition of nitrite and nitrate in oxygen-depleted waters cannot be explained without nitrite oxidation. The stoichiometry of nutrient remineralization indicates that most of the nitrite produced in OMZs is reoxidized *in situ* [18], which substantially decreases the loss of fixed nitrogen

Received: 23 April 2024. **Revised:** 29 July 2024. **Accepted:** 13 August 2024

in OMZs [14] and increases the retention of fixed nitrogen in the open ocean.

Nitrospinae are the most abundant NOB in the ocean and contribute to dark carbon fixation in deep, oxygenated waters [19]. Autotrophic carbon fixation, even using the efficient reductive TCA (rTCA) pathway conserved across all known *Nitrospinota* [20], requires the oxidation of large amounts of nitrite, which explains the finding that NXR enzymes affiliated with *Nitrospinae* are among the most abundant proteins in the ocean [21, 22]. NOB belonging to *Nitrospinae* Clade 1a and Clade 2 and *Nitrospirae* exhibited vertical, but not latitudinal, biogeography driven by differential adaptations to oxygen and nutrient conditions [19]. In OMZs, *Nitrospina* are the most common NOB, based on transcription of *nxr* [23], and nitrite oxidation rates in the Eastern Tropical South Pacific (ETSP) are correlated with *Nitrospina* 16S rRNA gene abundance [24].

Single-amplified genomes (SAGs) and metagenome-assembled genomes (MAGs) of NOB from globally distributed samples show no evidence of heterotrophy in marine *Nitrospinota* [19, 20]. A recent study comparing all known *Nitrospinota* from marine and freshwater sources illuminated the great diversity in the phylum and discovered genetic potential for the use of sulfide and hydrogen in some classes [20]. The particular *Nitrospinia* clades that are abundant in the ocean have not been cultured; their cultivated relatives are obligate aerobes and autotrophs [25], although lack of oxygen defense mechanisms and use of the rTCA cycle suggest microaerophilic ancestry.

The discovery of two Clade 1 *Nitrospina*-like NOB MAGs retrieved from the ETSP OMZ provided evidence that uncultured NOB may be responsible for nitrite oxidation in oxygen-depleted seawater. These MAGs (ETSP2013_BB2_MAG1 and ETSP2013_BB2_MAG2) reached relative abundances as high as 3% in the ODZ [26] and were found in published OMZ metatranscriptomes [23, 27], indicating activity and expression in the ODZs of the Eastern Tropical North Pacific (ETNP) and ETSP [14].

Our understanding of nitrite oxidation in OMZs, and its prevalence in oxygen-depleted waters, is hindered by our lack of understanding of the NOB responsible for this process in these regions. Here, we provide a comprehensive analysis of NOB communities in OMZs by identifying diverse NOB draft genomes (MAGs), exploring their metabolic repertoire, determining their distribution in OMZs and the global ocean, and quantifying the expression of *nxrB* genes. When combined with published nitrite oxidation rates obtained from the same samples, these multiple lines of evidence reveal specialist NOB that dominate oxygen-depleted waters and are responsible for high rates of nitrite oxidation.

Materials and methods

Metagenomic sequencing

Deep metagenomic sequencing was performed by the Joint Genome Institute (JGI) on 19 samples, 15 from depth profiles in the ETNP (Stations PS6 and 14 from 2016 and Stations PS2 and PS3 from 2018) and 4 from the Arabian Sea (Station 2 from 2007) (Tables S1 and S6), using a NovaSeq (Illumina). Analysis of the denitrifying community in a subset of these samples was recently reported [28]. Four of these ETNP stations (2016 station PS6, 2018 stations PS1, PS2, PS3) have previously published nitrite oxidation rates from the same exact samples; full details of these rate measurements can be found in [3, 15]. Full details of the cruises and sample collection were published previously [3, 14, 29]. Eight additional metagenomic samples (Table S1) were collected from the ETNP in 2018 at Stations PS2 and PS3 for a concurrent, currently unpublished, study. These additional eight samples were used only for binning MAGs; nitrite oxidation was not measured, and these samples are not included in the depth profiles. Details of the collection and processing of these samples can be found in supplemental methods. All metagenomic samples were collected on Sterivex (0.22 μm) filters, frozen immediately in liquid N_2 before being stored at −80°C, and extracted using the All-Prep DNA/RNA Mini Kit (Qiagen, Valencia, CA) and manufacturer's protocols.

Bioinformatics

Bioinformatic analyses were performed on a combination of the KBase [30] platform and Princeton University's High-Performance Computing servers. Sequences produced by JGI were quality controlled and trimmed by JGI protocols using BBDuk [31]. The remaining sequences were quality-controlled and trimmed using TrimGalore (https://github.com/FelixKrueger/TrimGalore) with a minimum quality score of 30, a stringency of 3, and a minimum length of 50.

Metagenomic reads from each sample were individually assembled using MEGAHIT v1.2.9 [32] with the meta-sensitive preset and a minimum contig length of 1000 bp. Each assembly was binned into MAGs using three separate binning programs, CONCOCT v1.1 [33], MaxBin2 v2.2.4 [34], and MetaBAT2 v1.7 [35]. Binning programs were set to accept a minimum contig length of 1000 bp except for MetaBAT2 (minimum contig length 1500 bp), and all programs used default settings with the exception that CONCOCT mapping was performed with bowtie2 very-sensitive presets. The resulting MAGs were dereplicated using DAS Tool v1.1.2 [36] to obtain a set of dereplicated MAGs for each sample. The quality of all MAGs was checked with CheckM v1.0.18 [37], and MAGs were taxonomically identified as NOB using GTDB-Tk v2.3.2 [38].

The average nucleotide identity (ANI) of each ODZ NOB MAG obtained from this study, calculated with FastANI [39], was compared to the other ODZ NOB and 61 dereplicated *Nitrospinota* genomes representing the full range of known marine *Nitrospinota* from cultures, MAGs, and SAGs (Table S3) [20]. ANI pairwise comparisons, which calculates ANI on shared regions of the genome and could therefore underestimate the true phylogenetic difference between distantly related organisms, were used to group NOB MAGs into species equivalents with a cutoff of 95% [40]. The best (highest-quality) MAG representing each species equivalent NOB group was chosen based on CheckM completion and contamination results with less contamination favored over a higher completeness for similar MAGs; representative MAGs (Table 1) for each group were substantially (>70%) or nearly (>90%) complete with medium (<10%) or better (<5%) contamination except for NOB6 and NOB8, which were moderately (>50%) complete (Table S2) [37]. These representative MAGs were used to calculate relative abundance for all ODZ NOB. In addition, representatives of *Nitrospinae* Clade 1a (AG-538-K21, called SAG_1a throughout), Clade 2a (AG-538-L21, called SAG_2a throughout), and *Nitrospirae* (AC-732-L14, called SAG_Nitrospirae throughout) are used to represent common NOB from oxygenated marine ecosystems (Table S3).

The number of reads in each sample that mapped to each NOB MAG was determined using bowtie2 [41], with very-sensitive presets and end-to-end alignment. All representative NOB MAGs and SAGs, as well as all cultured genomes, were mapped simultaneously, allowing each sample read to be mapped to only one genome. A modified version of RPKM (reads per kilobase per

Table 1. Completeness and contamination of each representative ODZ NOB MAG, and the sample from which each MAG was reconstructed.

NOB Group	MAG ID	Sample	Completeness (%)	Contamination (%)
ODZ NOB1	ODZ_NOB1a	ETNP PS3 70 m TF	96.5	5.2
ODZ NOB2	ODZ_NOB2a	ETNP PS6 200 m	97.2	5.1
ODZ NOB3	ODZ_NOB3a	ETNP PS6 750 m	84.2	3.5
ODZ NOB4	ODZ_NOB4a	ETNP 14185 m	94.6	8.8
ODZ NOB5	ODZ_NOB5a	ETNP PS2 130 m TF	82.0	7.5
ODZ NOB6	ODZ_NOB6a	ETNP PS2 130 m TF	56.6	1.9
ODZ NOB7	ODZ_NOB7a	Arabian Sea 150 m	95.7	1.7
ODZ NOB8	ODZ_NOB8a	Arabian Sea 150 m	67.9	6.7
ODZ NOB9	ODZ_NOB9a	Arabian Sea 200 m	71.9	3.5
ODZ NOB10	ODZ_NOB10a	Arabian Sea 400 m	91.0	1.7

million mapped reads) of each MAG in each sample was then determined by dividing the number of mapped reads by the total number of reads (in million) of the sample and dividing the resulting value by the genome length (kbp) of the MAG [42]. RPKM was used as a measure of relative abundance in order to normalize abundance to both sequencing depth and MAG length. The relative abundance of complete genomes of cultured organisms and previously identified NOB SAGs (Table S3) was determined following the same procedure. The representative NOBs were used to determine the relative abundance of the ODZ NOBs in additional samples from previously published studies (Table S4). NOB communities were compared using principal component analysis (PCoA) performed using phyloseq [43]. Pearson correlation analyses were performed using R [44] (α = 0.05) on samples with a complete set of data, i.e. stations PS6, PS2, and PS3. The relative abundance of cultured organisms was not included in the correlation analysis because many of the species had an RPKM of 0 across all samples.

A pangenome analysis was performed to better understand the genetic makeup of the most abundant and relatively closely related identified NOB, NOB1, NOB2, NOB3, and SAG_1a (AG_538_K21). The *Nitrospina gracilis* genome (strain 3/211) was included in the analysis as a well-characterized, complete genome comparison. The pangenome analysis was performed with anvi'o version 7.1 [45] using the anvi-pan-genome command and default settings; the programs DIAMOND [46] (with sensitive presets), HMMER [47], and prodigal [48] were utilized in the analysis. All ODZ NOB genomes, as well as *N. gracilis*, SAG_1a, and SAG_2a (AG_538_L21) were annotated with DRAM [49]; in addition, anvi'o was used to annotate each genome against the NCBI COGs, KEGG, and pfam databases [50–52]. Annotated genomes were used to search for specific genes of interest.

Quantification and phylogeny of *nxrB* genes

The beta subunit of the nitrite oxidoreductase gene (*nxrB*) is commonly used for NOB phylogeny and identification [53]; existing primer sets did not capture all the *nxrB* sequences identified from the OMZs so new primers were developed (see supplemental methods). The new primer set, nxrBomz1F (5' GAGTAYATGTGGTGGAAYAAYGT) and nxrBomz1R (5' CRTCCTCYTGGCGYTTGTA), was used to detect *nxrB* genes in the OMZ depth profiles with polymerase chain reaction (PCR) and quantitative PCR (qPCR).

SYBR green qPCR was performed to measure the number of *nxrB* gene copies in both DNA and cDNA (created from DNase I-treated RNA) of samples from the ETNP and Arabian Sea OMZs. Double-stranded cDNA was created using the Invitrogen (ThermoFisher, Waltham, MA) SuperScript III First-Strand Synthesis System and the Invitrogen Second-Strand cDNA Synthesis Kit following manufacturer protocols. The *nxrB* standard was diluted serially to make standard curves. Using optimized qPCR assays (see supplemental methods), each sample was run in triplicate and each plate included a negative control; a standard curve was accepted only if the $R^2 > 0.99$. No nonspecific binding was observed in gel electrophoresis of the amplified samples from PCR or qPCR.

To confirm the identity of NOB actively expressing *nxrB*, cDNA from the depth with the highest rate of nitrite oxidation from Stations PS6, PS1, PS2, and PS3 was cloned (see supplemental methods). Cloned *nxrB* nucleotide sequences were then aligned with *nxrB* sequences from metagenomes, cultured genomes, MAGs, and SAGs using MEGA [54] and their phylogenetic relationship to each other determined using IQ-Tree with default settings, 100 bootstraps, and model selection performed by IQ-Tree (best fit model: TNe + G4) [55]. Trees were visualized using iTOL version 6.6 [56].

Results

Nitrite-oxidizing bacteria from oxygen minimum zones

Samples from the ETNP and Arabian Sea OMZs (Table S1, Fig. S1, Fig. S6, supplemental discussion 1) were examined in search of new NOB draft genomes. Thirty-one MAGs, 51.89–97.31% (average 83.11%) completeness with contamination 1.71–14.01% (average 6.74%), were identified taxonomically as NOB (Table S2); 14 contained at least one copy of *nxrB* and 2 MAGs contained 2 copies. These ODZ NOB MAGs separated into 10 distinct groups (or "species," ANI cutoff 95%; Fig. 1). NOB1 consisted of 5 MAGs from the ETNP and 4 from the Arabian Sea and was the same as MAGs ETSP2013_BB2_NOB1, OceanDNA-b21315, and ERR599109_bin_11 previously binned from the OMZs of the ETSP, ETNP, and Arabian Sea, respectively (Fig. 1; Table S3). NOB2 included 5 NOB MAGs from the ETNP as well as the previously identified ETSP2013_BB2_NOB2. NOB3 included 3 MAGs from the ETNP; a fourth MAG from the Arabian Sea was included in this group despite its ANI of 90%, due to its low completeness (53%), further investigation may place this MAG in a separate group. NOB3 was the same as ERR599060_bin_7 isolated from the ETNP OMZ. The remaining NOB groups included 1 or 2 MAGs from the ENTP and Arabian Sea OMZs with NOB4 grouping with GEM_3300020338_10 from the ETNP OMZ, and NOB6 grouping with MAG ERR598946_bin_152 from the ETSP OMZ (Fig. 1). Each NOB group is represented by a representative

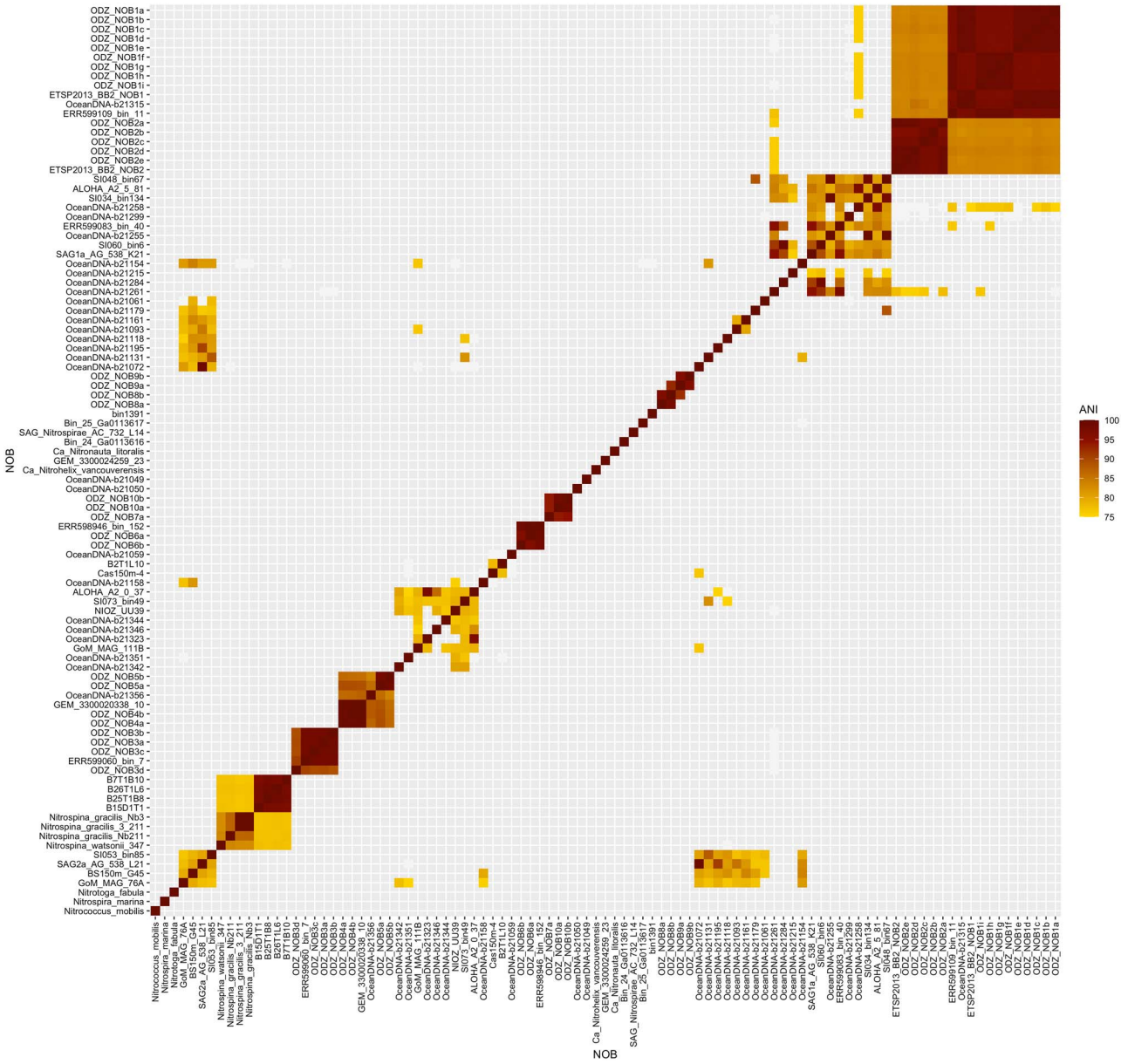

Figure 1. ANI (%) pairwise comparisons between NOB MAGs from this study and the genomes of previously published NOB MAGs, SAGs, and cultured NOB (Table S3). NOB groups were named for the NOB MAG from this study included in the group.

MAG (contamination <10%; Table 1) that is used for further analysis.

The ODZ NOB MAGs are only distantly related to cultured NOB and are different from NOB obtained from oxic marine waters and areas with seasonal ODZs like Saanich Inlet and the Gulf of Mexico (Fig. 1; Table S3). Based on GTDB-Tk taxonomy, NOB1, 2, and 3 fall into the class *Nitrospinia*, NOB4 and 5 belong to CAJXCL01 (previously UBA9942), NOB6 belongs to UBA7883, and NOB7, 8, 9, and 10 belong to UBA8248. UBA8248 has recently been re-categorized as its own phylum but was previously placed within *Nitrospinota* so these genomes were retained in the analysis. NOB1, 2, and 3 likely belong to *Nitrospinae* Clade 1, with NOB1 and 2 falling into Clade 1a. *nxrB*-based phylogeny confirms these results: *nxrB* genes from ODZ NOB MAGs were distinct from other *nxrB* genes except for those from *Nitrospinae* Clade 1a which were similar to NOB1 and 2, NOB4 and NOB5 *nxrB* genes group together, and genes isolated from NOB7, 8, and 10 group together on a more distant leaf (Fig. S2).

Abundance and activity of oxygen-deficient zone nitrite-oxidizing bacteria

All 10 ODZ NOB groups were present in all OMZ stations. Relative abundance (RPKM) of individual ODZ NOB groups ranged from zero in the upper, oxygenated surface waters to 6.85 RPKM (NOB3, 1.51% of total sequences) at 800 m in ETNP station PS3 (Fig. S3C). The combined RPKM of all ODZ NOB groups reached 15.37 RPKM (3.34% of the total sequences) in the ODZ of ETNP station 14 (Fig. 2, Fig. S3D). There was little difference in observed NOB communities between the ETNP and Arabian Sea OMZs, despite their large geographical distance, with NOB1, NOB2, and NOB3 dominating at ODZ depths. There were slightly higher relative abundances of NOB7, NOB8, and NOB9 in the Arabian Sea OMZ and slightly more NOB4 and NOB5 in the ETNP stations (Fig. S3). The distribution of individual ODZ NOB groups was similar between 2016 and 2018 in the ETNP, although NOB were more abundant in 2016.

ODZ NOB MAGs outnumbered any other identified NOB in all three major OMZs (Arabian Sea, ETNP, and ETSP) (Fig. 2, Fig. S3). In

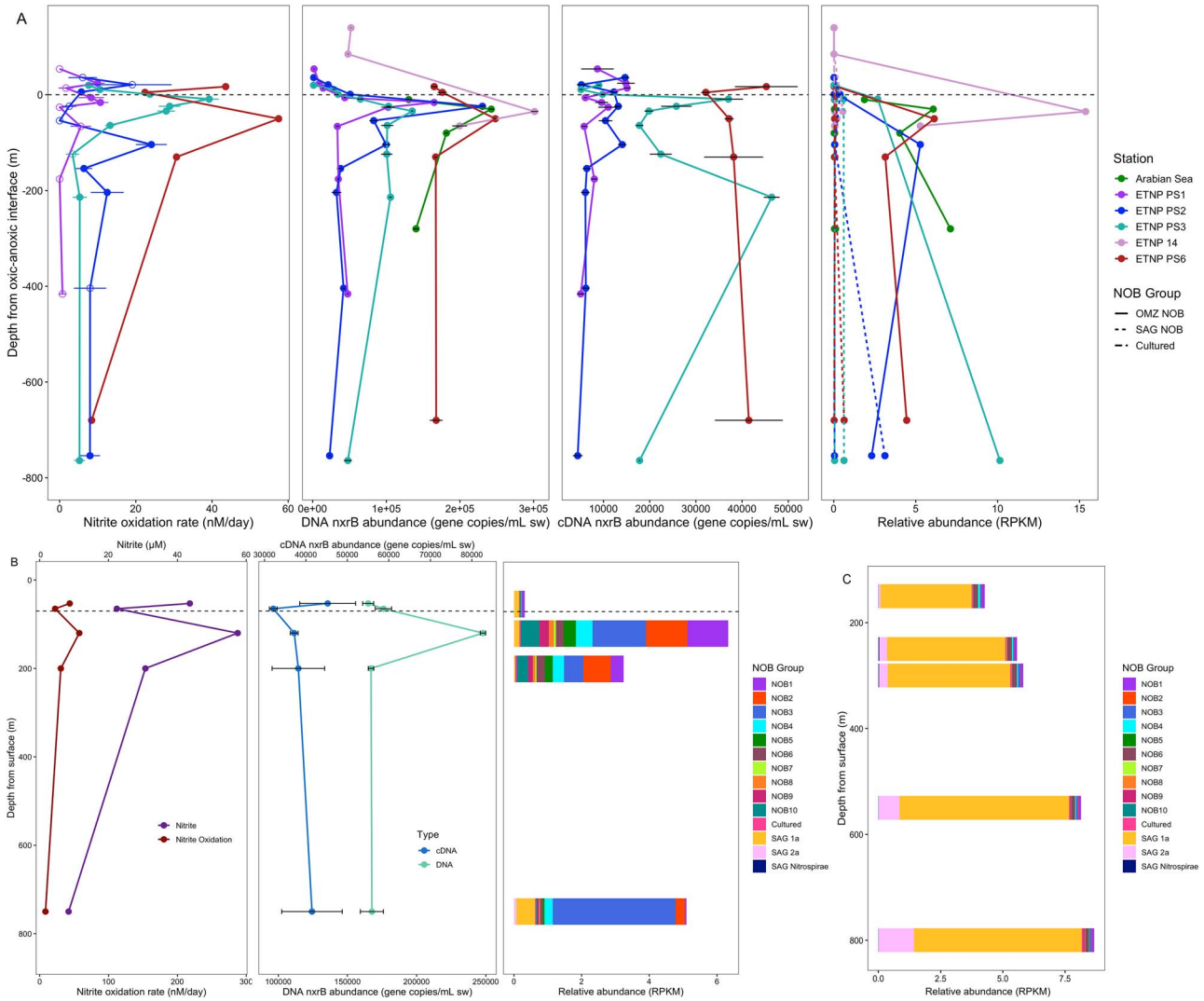

Figure 2. (A) The nitrite oxidation rate (nM/day, previously published in [3, 15]), DNA and cDNA based *nxrB* gene abundance (gene copies/mL seawater), and the relative abundance (RPKM) of NOB groups in each station plotted against the depth above (positive values) or below (negative values) the upper oxic-anoxic interface, defined as the depth where measured O_2 concentrations fell below 1 μmol/L across all stations (nitrite oxidation rates and cDNA not available for Arabian Sea and ETNP 14; relative abundance not available for ETNP PS1). RPKM shown here was calculated by combining the RPKM of the 10 representative ODZ NOB for the ODZ_NOB group, the 6 cultured organisms for cultured, and the 3 SAGs for SAG_NOB. Error bars represent standard error; nitrite oxidation error bars are from biological replicates, *nxrB* abundance error bars are from technical replicates. (B) The nitrite oxidation rate (nM/day), DNA and cDNA based *nxrB* gene abundance (gene copies/ml seawater), and the relative abundance (RPKM) of NOB in Station ETNP PS6, as an example, plotted against the depth (m) from the surface. (C) The relative abundance (RPKM) of NOB in an ETNP 2011 [21] station at the outer boundary of the OMZ where oxygen concentrations were above 10 μM at all depths; depth is plotted as meters from the surface.

general, NOB MAG relative abundance was minimal at the surface and increased in the ODZ, with all individual ODZ NOB MAGs peaking in the 200 m below the oxic-anoxic interface, except for NOB3, whose maximum relative abundance was deeper near the lower oxycline (Fig. 2). The only OMZ station where ODZ NOB MAGs did not dominate throughout the entire profile was ETNP PS2, where SAG_1a was abundant at the upper and lower oxyclines (Fig. S3B). The relative abundance of cultured NOB and SAG_Nitrospirae was negligible (0.01–0.07 and 0.02–0.06 RPKM, respectively) at all depths in all OMZ stations, as was SAG_2a, except for PS2 850 m.

ODZ NOB MAGs were obtained from the same samples (ETNP stations PS1, PS2, PS3, and PS6) as previously published nitrite oxidation rates, which ranged from 0–57.5 nM N/day [3, 15]. The highest rates occurred where no oxygen was detected *in situ*, roughly within the first 100 m below the upper oxycline (Fig. 2). At the non-ODZ station, PS1, nitrite oxidation rates were more variable with depth, though the highest rate occurred at the bottom of the oxycline (Fig. 2A, Fig. S3A). The potential density surface of $\sigma t = 26.4$ kg/m^3 is taken as the demarcation between the oxycline and ODZ core [6]. At all stations, the highest rates of nitrite oxidation occurred at depths shallower than or very close to $\sigma t = 26.4$ kg/m^3 although nitrite oxidation rates significantly greater than zero were observed at $\sigma t > 26.4$ (Fig. S4). Data on rates and metagenomes from the same samples allows a direct comparison of organisms and the processes attributed to them. At the depths of maximum nitrite oxidation, the nitrite-oxidizing community was dominated by NOB1, NOB2, and NOB3, with all other ODZ NOB present at lower abundances (Fig. 2, Fig. S3). Nitrite oxidation rates were significantly, positively correlated with the relative abundance of NOB1 ($r = 0.72$; Fig. 3, Fig. S5), and positively correlated with all other ODZ NOB relative abundance except for NOB3 and NOB4. There was a non-significant negative correlation between nitrite oxidation rates and SAG NOB abundances.

Using the new *nxrB* primers (see supplemental discussion 2, Fig. S7) for qPCR, *nxrB* gene abundance ranged from 1258 (±73,

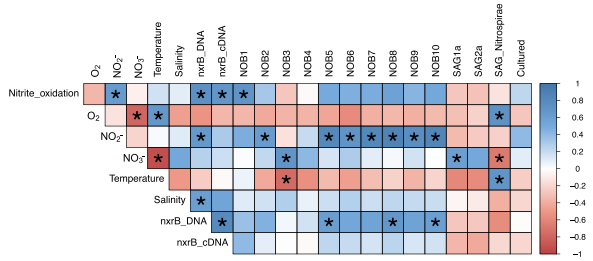

Figure 3. Pearson correlations comparing environmental variables and the RPKM of NOB groups from stations ETNP PS2, ETNP PS3, and ETNP PS6. A star (*) indicates a significant correlation ($P < 0.05$). Colors represent Pearson correlation value. Environmental variables include: Nitrite oxidation rates (Nitrite_oxidation), concentration of O_2, NO_2^-, NO_3^-, seawater temperature and salinity, the *nxrB* abundance based on DNA and cDNA, and the relative abundance (RPKM) of the each OMZ NOB group and each NOB SAG; cultured organisms were not included because some had zero relative abundance across all the included samples.

standard error) copies/mL in the surface waters of station PS3 to 301 326 (±4522) copies/mL in the ODZ of station 14 (Fig. 2; Fig. S3). The abundance of *nxrB* in cDNA was lower than in DNA, which is not surprising due to the rapid decay of RNA, from 4412 (±1000) copies/mL at 800 m at PS2 to 46 405 (±1661) copies/ml in the ODZ of PS3 (Fig. 2). *nxrB* expression levels may have been impacted by the sampling process despite filtering the samples as rapidly as possible and limiting oxygen exposure to the best of our abilities. *nxrB* abundance and relative abundance of NOB was higher in the 2016 ETNP stations (PS6 and 14) than in 2018 (PS2 and PS3). ETNP PS1, the station outside the OMZ, had the lowest abundance of *nxrB* genes and the lowest rates of nitrite oxidation (Fig. 2A).

Nitrite oxidation rates, *nxrB* abundance and expression, and ODZ NOB relative abundance, all obtained from the same samples, displayed similar depth profiles; all had maxima, often in the same samples, within 200 m below the oxic-anoxic interface where no oxygen was detected (Fig. 2A). *nxrB* abundance and expression were significantly ($P < 0.05$), positively correlated with each other ($r = 0.80$) and with nitrite oxidation rates ($r = 0.75$ and 0.70, respectively; Fig. 3). *nxrB* abundance and expression were positively correlated with ODZ NOB abundances, and negatively correlated with SAG NOB abundances (Fig. 3).

The position of sequences of expressed *nxrB* genes from stations PS1, PS2, PS3, and PS6 in the *nxrB* phylogenetic tree (Fig. S2) indicates that the active NOB were closely related to NOB1, NOB2, and SAG_1a. Therefore, the phylogeny of the cloned *nxrB* genes (see supplemental discussion 3) indicates that active NOB in ODZs are likely ODZ NOB MAGs, consistent with the metagenomic analysis.

Genetic potential of oxygen-deficient zone nitrite-oxidizing bacteria

The pangenome analysis of the most abundant ODZ NOB (NOB1, NOB2, and NOB3), the most abundant NOB from the oxygenated ocean (SAG_1a; AG_538_K21), and the complete genome of the closest cultivated relative (*N. gracilis* strain 3/211) identified 4692 gene clusters. Although each genome had unique gene clusters (not shared with any other genome), the five genomes shared a core set of just over 900 gene clusters (Fig. 4A; Table S5), which included all single copy housekeeping genes, the major genes for carbon fixation through the rTCA cycle previously observed in the *N. gracilis* genome [25], chlorite dismutase, and genes for the cytochrome bc complex and the F_0F_1-type ATP synthase. Nitrite oxidoreductase was not present in the core set because it was missing from the NOB3 genome; *nxr* from the other 4 examined genomes fell into the same gene cluster (Fig. 4A) and a different NOB3 genome did contain *nxrB* (Fig. 4B).

The ODZ NOB genomes shared some gene clusters that were not present in either SAG_1a or *N. gracilis*. NOB1 and NOB2 shared a group of about 100 clusters and all three ODZ NOB shared about 40 clusters (Fig. 4A, Table S5). Just under half of the gene clusters shared by ODZ NOB and not present in SAG_1a or *N. gracilis* were uncharacterized and their function could not be determined. The remaining gene clusters included genes for transcription and translation regulation, stress responses, ion transport and uptake, and energy metabolism, including a cbb3-type cytochrome oxidase, an NADPH nitrite reductase, and an NADPH:quinone reductase.

All ODZ NOB groups, as well as *N. gracilis* and both SAGs, contained the genes for cytochrome c oxidase, the high affinity cbb3-type cytochrome c oxidase, NADH:quinone oxidoreductase and, except for NOB9, cytochrome bd ubiquinol oxidase (Fig. 4B); no examined NOB had the lower affinity aa3-type oxidase or cytochrome o ubiquinol oxidase. The only ODZ NOB lacking *nxrB* were NOB6 and NOB9. Nitrite reductase (*nirK*) was present in NOB1, 2, 3, 4, 5, *N. gracilis*, and both SAGs. Nitrate reductase was present only in NOB1, 2, 3, and 8, and urease was present in NOB1, 2, 3, 7, and 10 (Fig. 4B). Unlike *N. gracilis*, ODZ NOB6, 7, 8, 9, and 10 contained a superoxide dismutase. Genes involved in sulfur cycling, including phosphoadenosine phosphosulfate reductase, sulfate adenylyltransferase, and sulfite reductase were present in the majority of the examined NOB genomes (Fig. 4B); genes for sulfur oxidation (i.e. *soxB*) were only found in NOB6. Only NOB5 contained genes for fumarate reductase.

Global biogeography of nitrite-oxidizing bacteria

The biogeography and relative abundance of the new ODZ NOB, previously reported NOB genomes and cultured representatives in 32 OMZ metagenomes (23 from this study, 9 previously published) and 23 previously published non-OMZ metagenomes representing major ocean biomes (Table S4), indicate clear niche separation between ODZ NOB and all other NOB. ODZ NOB MAGs were found in previously published OMZ metagenomes from the ETSP [26] and the ETNP (ETNP_2013) [57], with depth profiles similar to those reported here (Fig. 5A). Two ODZ NOB groups found in this study, NOB1 and NOB2, were the same "species" as NOB MAGs previously found in the ETSP OMZ; the relative abundance depth profile of NOB1 and NOB2 in the same ETSP metagenomes closely matched those previously reported (Fig. S3F) [14, 26]. All ODZ NOB groups were observed in very low abundances in metagenomes from just outside of the ETNP OMZ (ETNP_2011; Fig. 2C, 5A) [21] and were not detected in the oxygenated open ocean of the major ocean basins (Tara; Fig. 5A) [58].

The cultured NOB were negligible (0–0.09 RPKM) in all environmental samples (Fig. 5A). SAGs isolated from oxygenated mesopelagic zones [19] were present at the edges of the ODZ (upper and lower oxycline) in OMZ metagenome samples and were rarely detected in the ODZ (Fig. 5A, Fig. 2). SAG_1a was found in higher abundance in the oxygenated mesopelagic samples from all major ocean basins and in the entire depth profile from the non-OMZ ETNP metagenome (ETNP_2011) where it reached 6.81 RPKM, the equivalent of 1.73% of all sequenced reads, at 550 m (Fig. 2C). In contrast, the highest relative abundance of SAG_1a in an OMZ sample was 2.59 RPKM (Fig. 5A). SAG_2a was present in the same samples as SAG_1a, but at lower abundance; SAG_Nitrospirae was present in only a few metagenomes at very low abundances (Fig. 5A).

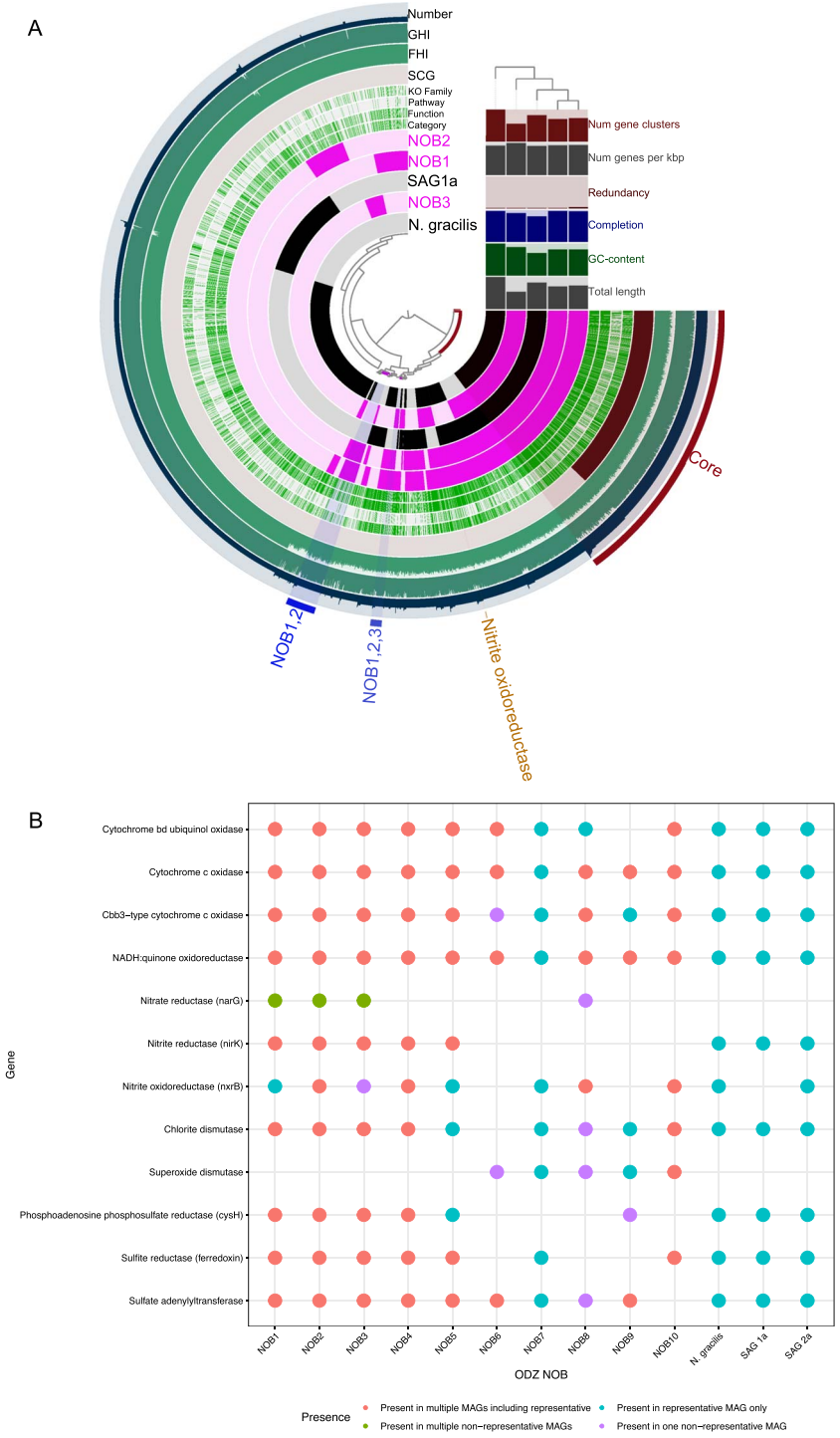

Figure 4. (A) Pangenomic analysis of gene clusters present in ODZ NOBs NOB1, NOB2, NOB3, as well as SAG1a (AG-538-K21, IMG genome 2681812871) and *N. gracilis* strain 3/211 (NCBI: SAMEA2272521) genomes. Gene clusters shared across all five genomes are labeled Core; gene clusters shared across NOB1 and NOB2 genomes are labeled NOB1,2 and across all three ODZ NOBs are labeled NOB1,2,3. The location of the nitrite oxidoreductase gene cluster is also indicated. Layers of the figure are, from top to bottom, the number of genes in the gene cluster (Number), the geometric homogeneity index (GHI), the functional homogeneity index (FHI), the presence of single copy gene (SCG) clusters, the KO family, the COG20 pathway (Pathway), the COG20 function (Function), the COG20 category (Category), the presence of a gene cluster in NOB2, NOB1, SAG1a, NOB3, and *N. gracilis*. For the KO family and the COG20 layers, known is shown in green and unknown is shown in white. Included in the bar graphs are the number of gene clusters, number of genes per kilobasepair, redundancy, completion, GC content, and total length of each genome. (B) The presence (dot present) or absence (no dot present) of genes of interest in each of the ODZ NOB groups, *N. gracilis*, SAG1a, and SAG2a (AG-538-L21, IMG genome 2681812872). Color of the dot represents the number of MAGs the gene was present in.

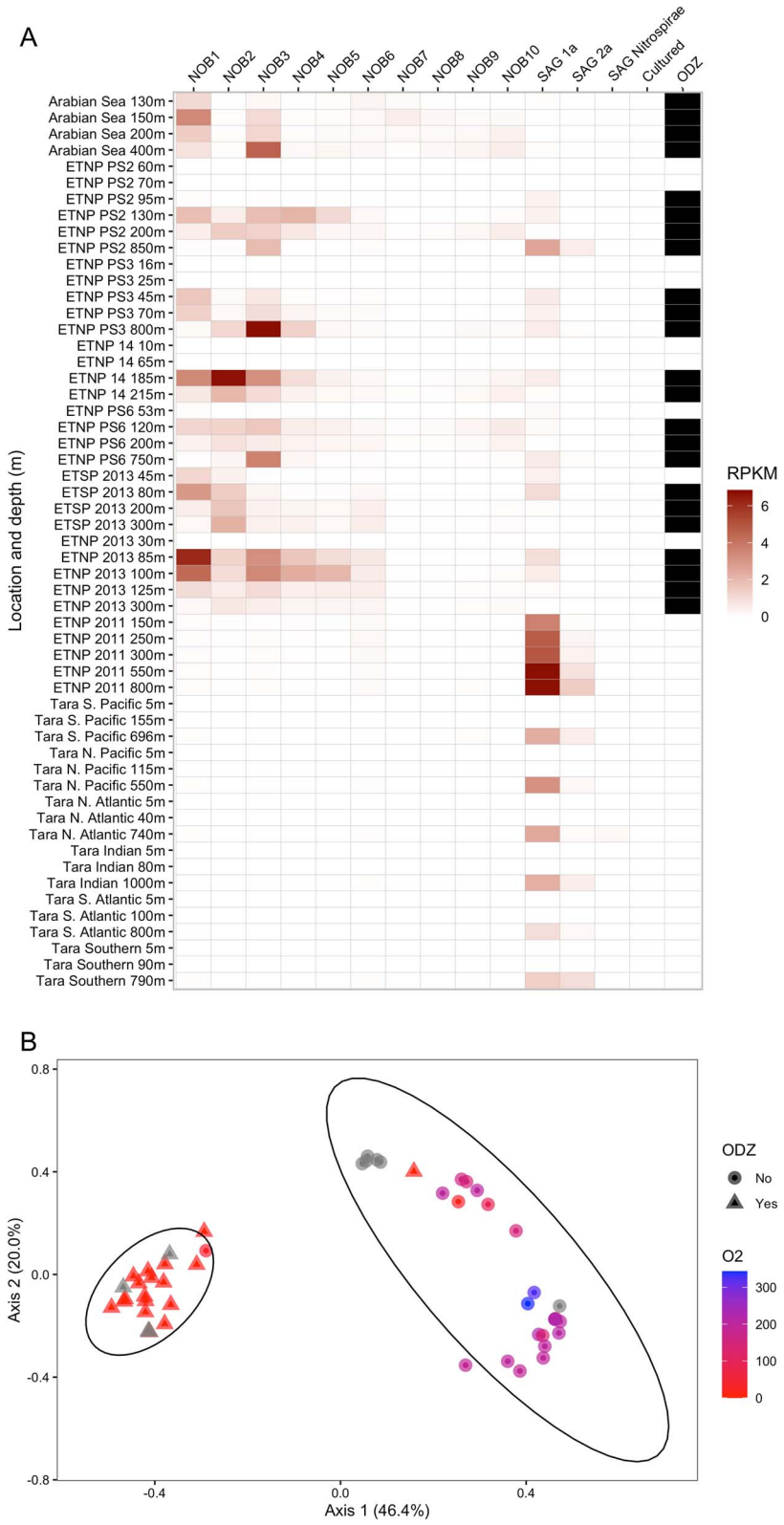

Figure 5. (A) Relative abundance (RPKM) of NOB in metagenomes from this study and previous studies (see Tables S1 and S4). ODZ indicates the sample location in the ODZ (black, <10 μM O_2) or outside the ODZ (white, >10 μM O_2). NOB and SAG groups are represented by their associated representative genome (see Tables S2 and S3); cultured NOB is the average RPKM of all considered cultured NOB. (B) A PCoA of the NOB communities, based on RPKM, in each sample. Shape represents whether the sample came from an ODZ (<10 μM O_2) or not (>10 μM O_2); color represents the O_2 concentration. Gray was used when the exact O_2 concentration was unknown. Data ellipses were calculated using a multivariate *t*-distribution.

A PCoA based on relative abundance of all NOB genomes, MAGs, and SAGs separated the NOB communities into two major groups, one at higher oxygen levels (including upper and lower oxycline samples), and the second from ODZs (Fig. 5B). The ODZ group of communities included samples from this study and from the ODZ of the ETNP_2013 and ETSP_2013 [26, 57]; the other group included all samples from the oxygenated open ocean [58] as well as samples from OMZ upper and lower oxyclines and the outer boundary of an OMZ (ETNP_2011) [21]. A smaller component of the variability among communities was associated with depth, with shallower samples separating from deeper mesopelagic samples. This is particularly evident in the oxygenated samples (Fig. 5B), which separated between surface and mesopelagic. The separation of NOB communities by environmental (oxygen and depth) factors rather than by station or geographic region supports the idea that NOB present in ODZs are uniquely adapted to that environment, regardless of the geographic location of the OMZ.

Discussion

Oxygen-deficient zones harbor a distinct community of nitrite-oxidizing bacteria

Thirty-one NOB MAGs belonging to 10 different "species" were identified from OMZ metagenomes. The most abundant NOB belonged to the class *Nitrospinia*, consistent with the dominance of *Nitrospina* in previous reports from ETNP and global oceans [7, 19, 21, 23]. The ODZ NOB groups are distinct from cultured NOB and NOB previously identified to be important in the open ocean [19]. Several Clade 1 *Nitrospina*-like organisms, including SAG_1a (AG-538-K21), have been grouped into a suggested genus, *Candidatus* Nitromaritima, which was phylogenetically distinct from *N. gracilis* and abundant in the ETSP OMZ and the Red Sea [59]. The high diversity of NOB present in OMZs and their distant phylogenetic relationship to other NOB suggest that nitrite oxidizers are more diverse than previously recognized, supporting the conclusions of a recent analysis of the *Nitrospinota* phylum [20]. ODZ NOB were only closely related to other NOB from OMZ regions, not to NOB from oxic or seasonally anoxic regions, implying that these ODZ NOB are adapted specifically to permanently oxygen-depleted environments.

The clear contrast between distribution of NOB at OMZ vs. open ocean stations indicates strong niche separation in NOB communities with ODZ NOB MAGs specializing in ODZ environments. The pangenomic and genome-based analyses identified a core genetic component shared between ODZ and non-ODZ NOB with a smaller subset of genes unique to each group and to individual species. Based on the shared similarity in core metabolic functions, both ODZ and non-ODZ NOB are likely to be able to function as aerobes. Some genes, like the high-affinity cbb3-type cytochrome c oxidase [60], likely support NOB growth in low-oxygen waters; the existence of these genes in both ODZ NOB and NOB from oxic systems shows that the evolutionary advantage of these microaerophilic adaptations exists outside of the ODZ. The pangenome comparison revealed cbb3-type cytochrome c oxidase and other energy metabolism genes belonged to different gene clusters in the ODZ NOB and SAG_1a and *N. gracilis*, potentially implying a gene-level variation in these key enzymes, though more research into these and other shared genes is needed to determine if these gene-level variations result in functional changes. Although there are no obvious gene clusters that enable the ODZ MAGs to survive and outcompete other NOBs in the ODZs, the presence of gene clusters unique to ODZ MAGs supports their genetic distinction from other NOB and may in the future provide clues to the specific adaptations of ODZ NOBs, especially as currently unknown proteins are characterized.

The genome analysis of ODZ MAGs supports many of the findings from the recent investigation into the *Nitrospinota* phylum including the presence of *nirK* and urease in *Nitrospinia* MAGs, the presence of *soxB* in class UBA7883 (NOB6) and a potential role of *Nitrospinota* in sulfur cycling, and the conservation of autotrophic growth by the rTCA cycle across all *Nitrospinota* genomes [20]. Recent research has also suggested that the class *Nitrospinia* are the most abundant and active nitrite oxidizers in the ocean and that other *Nitrospinota* may play other roles [20], though more research needs to be done to evaluate this hypothesis. The *Nitrospinia* ODZ MAGs (i.e. NOB 1, 2, and 3) were the most dominant ODZ NOB and NOB1 and 2 had the closest relationship with nitrite oxidation rates in the OMZs. Although these genome-based analyses can provide valuable information on the potential roles of these organisms, further research is required to understand the controls on these genomes in the marine environments and which genes are tied to their survival in the ODZ niche. This work provides the first step in better understanding the ODZ NOB by exploring their global biogeography and linking their presence to activity in the ODZ.

Oxygen-deficient zone nitrite-oxidizing bacteria are responsible for nitrite oxidation in oxygen-depleted waters

The highest rates of nitrite oxidation in OMZs are consistently reported in oxygen-depleted waters, though experimental oxygen manipulation experiments document variable responses of nitrite oxidation to oxygen [1, 3, 6, 7, 10, 61, 62]. The rates represented in this paper are no exception, with the highest nitrite oxidation rate occurring in the ODZ in all stations, generally coinciding with the highest abundance and expression of *nxrB*. The strong correlation between nitrite oxidation and *nxrB* abundance and expression, even considering that the *nxrB* abundance may overestimate the cell number because *nxrB* often occurs in two copies in *Nitrospina* genomes [25], supports the idea that nitrite oxidation is actively being performed by NOB in the ODZ. The high identity between *nxrB* from ODZ NOB and *nxrB* cloned from cDNA at the nitrite oxidation peak (see supplemental discussion 3) shows that the NOB performing the nitrite oxidation are the newly identified ODZ NOB. Furthermore, the strong correlation between the relative abundance of ODZ NOB, especially NOB1, and nitrite oxidation rates adds additional support for identity of the active members of the NOB community. Overall, the biogeochemical and molecular analyses from the same samples indicate that the ODZ NOB MAGs represent the primary organisms responsible for nitrite oxidation in ODZ waters; the NOB SAGs previously identified to be critical for marine nitrite oxidation [19] are only prevalent in oxygenated waters.

Many mechanisms have previously been proposed to explain apparently anaerobic nitrite oxidation, i.e. nitrite oxidation that occurs in oxygen-depleted waters, including: (i) canonical aerobic nitrite oxidation supported by sporadic intrusions of oxygen [63], (ii) use of an alternative electron acceptor such as iodate [10], (iii) nitrite dismutation [64], (iv) isotopic equilibration catalyzed by the reversible NXR protein, resulting in isotopic enrichment of the nitrate pool without net production of nitrate [65–67], and (v) cryptic oxygen cycling between *Prochlorococcus* and NOB at the deep chlorophyll maximum [67]. A full discussion of these suggested explanations and their relevance to the observed nitrite oxidation in OMZs has recently been published [8].

More recent modeling work has suggested that infrequent oxygen intrusions could support high rates of aerobic nitrite oxidation [68]. Although no oxygen intrusions were detected in STOX sensor profiles during sample collection, the highest ODZ NOB abundances, nitrite oxidation rates, and gene expression abundance occurred at depths shallower than or close to $\sigma t = 26.4$ kg/m^3. At depths shallower than $\sigma t = 26.4$, intrusions of oxygen are considered possible, if infrequent; at deeper depths, significant impact of such intrusions is considered negligible [4]. This is also the depth where, based on the stoichiometry of organic matter remineralization, >50% of the nitrite produced in the OMZ is reoxidized [18].

The exact mechanism behind nitrite oxidation in the absence of detectable oxygen needs further study, but the presence of microaerobic core metabolism in ODZ NOB suggests that infrequent intrusions of oxygen-bearing water [68] are the most likely explanation. Anaerobic metabolism cannot be ruled out, however, as further analysis of uncharacterized genes present in ODZ NOB MAGs may reveal unknown functions. The ODZ NOB are responsible for nitrite oxidation in the apparent absence of oxygen and therefore for the retention of fixed nitrogen in OMZs. Further exploration of their genomes may reveal the adaptations that make them unique from all other NOB and allow them to exploit and dominate this niche.

Acknowledgements

The authors would like to thank Galen Cadley for her assistance identifying *nxrB* genes in ETNP metagenomes. This publication was supported by the Princeton University Library Open Access Fund.

Author contributions

Samantha G. Fortin (Conceptualization, Methodology, Investigation, Visualization, Writing—original draft, Writing—review & editing), Xin Sun (Conceptualization, Methodology, Investigation, Writing—review & editing), Amal Jayakumar (Methodology, Investigation, Supervision, Writing—review & editing), and Bess B. Ward (Conceptualization, Investigation, Visualization, Funding acquisition, Project administration, Supervision, Writing—original draft, Writing—review & editing)

Supplementary material

Supplementary material is available at *The ISME Journal* online.

Conflicts of interest

None declared.

Funding

National Science Foundation grant 1657663 (B.B.W.). National Science Foundation grant 1946516 (B.B.W.). Simons Foundation grant 675459 (B.B.W).

Data and materials availability

Metagenomic data and MAGs used in this study are available at JGI (Proposal ID 503962) and NCBI (BioProject PRJNA1003508). More information on the ETNP 2018 samples can be found in BCO-DMO project 741 018. Code used in this analysis can be found at https://github.com/sgfortin/ODZ-NOB.

References

1. Lipschultz F, Wofsy SC, Ward BB *et al.* Bacterial transformations of inorganic nitrogen in the oxygen-deficient waters of the eastern tropical South Pacific Ocean. *Deep-Sea Res* 1990;**37**:1513–41. https://doi.org/10.1016/0198-0149(90)90060-9
2. Füssel J, Lücker S, Yilmaz P *et al.* Adaptability as the key to success for the ubiquitous marine nitrite oxidizer Nitrococcus. *Sci Adv* 2017;**3**:e1700807. https://doi.org/10.1126/sciadv.1700807
3. Sun X, Ji Q, Jayakumar A *et al.* Dependence of nitrite oxidation on nitrite and oxygen in low-oxygen seawater. *Geophys Res Lett* 2017;**44**:7883–91. https://doi.org/10.1002/2017GL074355
4. Babbin AR, Buchwald C, Morel FMM *et al.* Nitrite oxidation exceeds reduction and fixed nitrogen loss in anoxic Pacific waters. *Mar Chem* 2020;**224**:103814. https://doi.org/10.1016/j.marchem.2020.103814
5. Moore CM, Mills MM, Arrigo KR *et al.* Processes and patterns of oceanic nutrient limitation. *Nat Geosci* 2013;**6**:701–10. https://doi.org/10.1038/ngeo1765
6. Peng X, Fuchsman CA, Jayakumar A *et al.* Ammonia and nitrite oxidation in the eastern tropical North Pacific. *Glob Biogeochem Cycles* 2015;**29**:2034–49. https://doi.org/10.1002/2015GB005278
7. Beman JM, Leilei Shih J, Popp BN. Nitrite oxidation in the upper water column and oxygen minimum zone of the eastern tropical North Pacific Ocean. *ISME J* 2013;**7**:2192–205. https://doi.org/10.1038/ismej.2013.96
8. Sun X, Frey C, Ward BB. Nitrite oxidation across the full oxygen spectrum in the ocean. *Glob Biogeochem Cycles* 2023;**37**:e2022GB007548. https://doi.org/10.1029/2022GB007548
9. Bristow LA, Dalsgaard T, Tiano L *et al.* Ammonium and nitrite oxidation at nanomolar oxygen concentrations in oxygen minimum zone waters. *Proc Natl Acad Sci* 2016;**113**:10601–6. https://doi.org/10.1073/pnas.1600359113
10. Babbin AR, Peters BD, Mordy CW *et al.* Multiple metabolisms constrain the anaerobic nitrite budget in the eastern tropical South Pacific. *Glob Biogeochem Cycles* 2017;**31**:258–71. https://doi.org/10.1002/2016GB005407
11. Füssel J, Lam P, Lavik G *et al.* Nitrite oxidation in the Namibian oxygen minimum zone. *ISME J* 2012;**6**:1200–9. https://doi.org/10.1038/ismej.2011.178
12. van de Vossenberg J, Woebken D, Maalcke WJ *et al.* The metagenome of the marine anammox bacterium 'Candidatus Scalindua profunda' illustrates the versatility of this globally important nitrogen cycle bacterium. *Environ Microbiol* 2012;**15**:1275–89. https://doi.org/10.1111/j.1462-2920.2012.02774.x
13. Chicano TM, Dietrich L, de Almeida NM *et al.* Structural and functional characterization of the intracellular filament-forming nitrite oxidoreductase multiprotein complex. *Nat Microbiol* 2021;**6**:1129–39. https://doi.org/10.1038/s41564-021-00934-8
14. Sun X, Frey C, Garcia-Robledo E *et al.* Microbial niche differentiation explains nitrite oxidation in marine oxygen minimum zones. *ISME J* 2021;**15**:1317–29. https://doi.org/10.1038/s41396-020-00852-3
15. Tracey JC, Babbin AR, Wallace E *et al.* All about nitrite: exploring nitrite sources and sinks in the eastern tropical North Pacific oxygen minimum zone. *Biogeosciences* 2023;**20**:2499–523. https://doi.org/10.5194/bg-20-2499-2023
16. Casciotti KL, Buchwald C, McIlvin M. Implications of nitrate and nitrite isotopic measurements for the mechanisms of nitrogen cycling in the Peru oxygen deficient zone. *Deep Sea Res 1 Oceanogr Res Pap* 2013;**80**:78–93. https://doi.org/10.1016/j.dsr.2013.05.017
17. Peters BD, Babbin AR, Lettmann KA *et al.* Vertical modeling of the nitrogen cycle in the eastern tropical South Pacific oxygen

deficient zone using high-resolution concentration and isotope measurements. *Glob Biogeochem Cycles* 2016;**30**:1661–81. https://doi.org/10.1002/2016GB005415
18. Evans N, Tichota J, Moffett JW *et al.* Prolific nitrite reoxidation across the eastern tropical North Pacific Ocean. *Limnol Oceanogr* 2023;**68**:1719–33. https://doi.org/10.1002/lno.12380
19. Pachiadaki MG, Sintes E, Bergauer K *et al.* Major role of nitrite-oxidizing bacteria in dark ocean carbon fixation. *Science* 2017;**358**:1046–51. https://doi.org/10.1126/science.aan8260
20. Kop LFM, Koch H, Jetten MSM *et al.* Metabolic and phylogenetic diversity in the phylum Nitrospinota revealed by comparative genome analyses. *ISME Commun* 2024;**4**:ycad017. https://doi.org/10.1093/ismeco/ycad017
21. Saito MA, McIlvin MR, Moran DM *et al.* Abundant nitrite-oxidizing metalloenzymes in the mesopelagic zone of the tropical Pacific Ocean. *Nat Geosci* 2020;**13**:355–62. https://doi.org/10.1038/s41561-020-0565-6
22. Saunders JK, Mcilvin MR, Dupont CL *et al.* Microbial functional diversity across biogeochemical provinces in the Central Pacific Ocean. *Proc Natl Acad Sci* 2022;**119**:e2200014119. https://doi.org/10.1073/pnas.2200014119
23. Ganesh S, Bristow LA, Larsen M *et al.* Size-fraction partitioning of community gene transcription and nitrogen metabolism in a marine oxygen minimum zone. *ISME J* 2015;**9**:2682–96. https://doi.org/10.1038/ismej.2015.44
24. Santoro AE, Buchwald C, Knapp AN *et al.* Nitrification and nitrous oxide production in the offshore waters of the eastern tropical South Pacific. *Glob Biogeochem Cycles* 2021;**35**:e2020GB006716. https://doi.org/10.1029/2020GB006716
25. Lücker S, Nowka B, Rattei T *et al.* The genome of Nitrospina gracilis illuminates the metabolism and evolution of the major marine nitrite oxidizer. *Front Microbiol* 2013;**4**:00027. https://doi.org/10.3389/fmicb.2013.00027
26. Sun X, Kop LFM, Lau MCY *et al.* Uncultured Nitrospina-like species are major nitrite oxidizing bacteria in oxygen minimum zones. *ISME J* 2019;**13**:2391–402. https://doi.org/10.1038/s41396-019-0443-7
27. Stewart FJ, Ulloa O, Delong EF. Microbial metatranscriptomics in a permanent marine oxygen minimum zone. *Environ Microbiol* 2012;**14**:23–40. https://doi.org/10.1111/j.1462-2920.2010.02400.x
28. Zhang IH, Sun X, Jayakumar A *et al.* Partitioning of the denitrification pathway and other nitrite metabolisms within global oxygen deficient zones. *ISME Commun* 2023;**3**:76. https://doi.org/10.1038/s43705-023-00284-y
29. Ward BB, Devol AH, Rich JJ *et al.* Denitrification as the dominant nitrogen loss process in the Arabian Sea. *Nature* 2009;**461**:78–81. https://doi.org/10.1038/nature08276
30. Arkin AP, Cottingham RW, Henry CS *et al.* KBase: the United States Department of Energy Systems Biology Knowledgebase. *Nat Biotechnol* 2018;**36**:566–9. https://doi.org/10.1038/nbt.4163
31. Bushnell B. bbMap: a fast, accurate, splice-aware aligner. *Conference: 9th Annual Genomics of Energy & Environment Meeting,* United States, N. p., 2014.
32. Li D, Liu CM, Luo R *et al.* MEGAHIT: an ultra-fast single-node solution for large and complex metagenomics assembly via succinct de Bruijn graph. *Bioinformatics* 2015;**31**:1674–6. https://doi.org/10.1093/bioinformatics/btv033
33. Alneberg J, Bjarnason BS, de Bruijn I *et al.* Binning metagenomic contigs by coverage and composition. *Nat Methods* 2014;**11**:1144–6. https://doi.org/10.1038/nmeth.3103
34. Wu YW, Tang YH, Tringe SG *et al.* MaxBin: an automated binning method to recover individual genomes from metagenomes using an expectation-maximization algorithm. *Microbiome* 2014;**2**:26. https://doi.org/10.1186/2049-2618-2-26
35. Kang DD, Li F, Kirton E *et al.* MetaBAT2: an adaptive binning algorithm for robust and efficient genome reconstruction from metagenome assemblies. *PeerJ* 2019;**7**:e7359. https://doi.org/10.7717/peerj.7359
36. Sieber CMK, Probst AJ, Sharrar A *et al.* Recovery of genomes from metagenomes via a dereplication, aggregation and scoring strategy. *Nat Microbiol* 2018;**3**:836–43. https://doi.org/10.1038/s41564-018-0171-1
37. Parks DH, Imelfort M, Skennerton CT *et al.* CheckM: assessing the quality of microbial genomes recovered from isolates, single cells, and metagenomes. *Genome Res* 2015;**25**:1043–55. https://doi.org/10.1101/gr.186072.114
38. Chaumeil P, Mussig A, Hugenholtz P *et al.* GTDB-Tk: a toolkit to classify genomes with the genome taxonomy database. *Bioinformatics* 2019;**36**:1925–7. https://doi.org/10.1093/bioinformatics/btz848
39. Jain C, Rodriguez-R LM, Phillippy AM *et al.* High throughput ANI analysis of 90K prokaryotic genomes reveals clear species boundaries. *Nat Commun* 2018;**9**:5114. https://doi.org/10.1038/s41467-018-07641-9
40. Konstantinidis KT, Tiedje JM. Genomic insights that advance the species definition for prokaryotes. *Proc Natl Acad Sci* 2005;**102**:2567–72. https://doi.org/10.1073/pnas.0409727102
41. Langmead B, Salzberg SL. Fast gapped-read alignment with bowtie 2. *Nat Methods* 2012;**9**:357–9. https://doi.org/10.1038/nmeth.1923
42. Sevillano M, Dai Z, Calus S *et al.* Differential prevalence and host-association of antimicrobial resistance traits in disinfected and non-disinfected drinking water systems. *Sci Total Environ* 2020;**749**:141451. https://doi.org/10.1016/j.scitotenv.2020.141451
43. McMurdie PJ, Holmes S. Phyloseq: an R package for reproducible interactive analysis and graphics of microbiome census data. *PLoS One* 2013;**8**:e61217. https://doi.org/10.1371/journal.pone.0061217
44. R Core Team. R: A language and environment for statistical computing. *R Foundation for Statistical Computing*. Vienna: Austria, 2018.
45. Eren AM, Kiefl E, Shaiber A *et al.* Community-led, integrated, reproducible multi-omics with anvi'o. *Nat Microbiol* 2021;**6**:3–6. https://doi.org/10.1038/s41564-020-00834-3
46. Buchfink B, Xie C, Huson DH. Fast and sensitive protein alignment using DIAMOND. *Nat Methods* 2014;**12**:59–60. https://doi.org/10.1038/nmeth.3176
47. Eddy SR. Accelerated profile HMM searches. *PLoS Comput Biol* 2011;**7**:e1002195. https://doi.org/10.1371/journal.pcbi.1002195
48. Hyatt D, Chen G-L, Locascio PF *et al.* Prodigal: prokaryotic gene recognition and translation initiation site identification. *BMC Bioinformatics* 2010;**11**:119. https://doi.org/10.1186/1471-2105-11-119
49. Shaffer M, Borton MA, McGivern BB *et al.* DRAM for distilling microbial metabolism to automate the curation of microbiome function. *Nucleic Acids Res* 2020;**48**:8883–900. https://doi.org/10.1093/nar/gkaa621
50. Mistry J, Chuguransky S, Williams L *et al.* Pfam: the protein families database in 2021. *Nucleic Acids Res* 2021;**49**:D412–9. https://doi.org/10.1093/nar/gkaa913
51. Galperin MY, Makarova KS, Wolf YI *et al.* Expanded microbial genome coverage and improved protein family annotation in the COG database. *Nucleic Acids Res* 2015;**43**:D261–9. https://doi.org/10.1093/nar/gku1223
52. Kanehisa M, Goto S. KEGG: Kyoto Encyclopedia of genes and genomes. *Nucleic Acids Res* 2000;**28**:27–30. https://doi.org/10.1093/nar/28.1.27

53. Pester M, Maixner F, Berry D *et al.* NxrB encoding the beta subunit of nitrite oxidoreductase as functional and phylogenetic marker for nitrite-oxidizing Nitrospira. *Environ Microbiol* 2014;**16**:3055–71. https://doi.org/10.1111/1462-2920.12300
54. Tamura K, Peterson D, Peterson N *et al.* MEGA5: molecular evolutionary genetics analysis using maximum likelihood, evolutionary distance, and maximum parsimony methods. *Mol Biol Evol* 2011;**28**:2731–9. https://doi.org/10.1093/molbev/msr121
55. Trifinopoulos J, Nguyen LT, von Haeseler A *et al.* W-IQ-TREE: a fast online phylogenetic tool for maximum likelihood analysis. *Nucleic Acids Res* 2016;**44**:W232–5. https://doi.org/10.1093/nar/gkw256
56. Letunic I, Bork P. Interactive tree of life (iTOL): an online tool for phylogenetic tree display and annotation. *Bioinformatics* 2006;**23**:127–8. https://doi.org/10.1093/bioinformatics/btl529
57. Glass JB, Kretz CB, Ganesh S *et al.* Meta-omic signatures of microbial metal and nitrogen cycling in marine oxygen minimum zones. *Front Microbiol* 2015;**6**:00998. https://doi.org/10.3389/fmicb.2015.00998
58. Sunagawa S, Coelho LP, Chaffron S *et al.* Structure and function of the global ocean microbiome. *Science* 2015;**348**:1261359. https://doi.org/10.1126/science.1261359
59. Ngugi DK, Blom J, Stepanauskas R *et al.* Diversification and niche adaptations of Nitrospina-like bacteria in the polyextreme interfaces of Red Sea brines. *ISME J* 2016;**10**:1383–99. https://doi.org/10.1038/ismej.2015.214
60. Han H, Hemp J, Pace LA *et al.* Adaptation of aerobic respiration to low O2 environments. *Proc Natl Acad Sci* 2011;**108**:14109–14. https://doi.org/10.1073/pnas.1018958108
61. Beman JM, Vargas SM, Wilson JM *et al.* Substantial oxygen consumption by aerobic nitrite oxidation in oceanic oxygen minimum zones. *Nat Commun* 2021;**12**:7043. https://doi.org/10.1038/s41467-021-27381-7
62. Peng X, Fuchsman CA, Jayakumar A *et al.* Revisiting nitrification in the Eastern Tropical South Pacific: a focus on controls. *J Geophys Res Oceans* 2016;**121**:1667–84. https://doi.org/10.1002/2015JC011455
63. Thamdrup B, Dalsgaard T, Revsbech NP. Widespread functional anoxia in the oxygen minimum zone of the Eastern South Pacific. *Deep Sea Res 1 Oceanogr Res Pap* 2012;**65**:36–45. https://doi.org/10.1016/j.dsr.2012.03.001
64. Ettwig KF, Butler MK, Le Paslier D *et al.* Nitrite-driven anaerobic methane oxidation by oxygenic bacteria. *Nature* 2010;**464**:543–8. https://doi.org/10.1038/nature08883
65. Wunderlich A, Meckenstock RU, Einsiedl F. A mixture of nitrite-oxidizing and denitrifying microorganisms affects the δ18O of dissolved nitrate during anaerobic microbial denitrification depending on the δ18O of ambient water. *Geochim Cosmochim Acta* 2013;**119**:31–45. https://doi.org/10.1016/j.gca.2013.05.028
66. Kemeny PC, Weigand MA, Zhang R *et al.* Enzyme-level interconversion of nitrate and nitrite in the fall mixed layer of the Antarctic Ocean. *Glob Biogeochem Cycles* 2016;**30**:1069–85. https://doi.org/10.1002/2015GB005350
67. Buchwald C, Wankel SD. Enzyme-catalyzed isotope equilibrium: a hypothesis to explain apparent N cycling phenomena in low oxygen environments. *Mar Chem* 2022;**244**:104140. https://doi.org/10.1016/j.marchem.2022.104140
68. Buchanan PJ, Sun X, Weissman JL *et al.* Oxygen intrusions sustain aerobic nitrite oxidation in anoxic marine zones. *bioRxiv* 2023. https://doi.org/10.1101/2023.02.22.529547

Supporting information for

Low oxygen specialist nitrite oxidizing bacteria dominate nitrite oxidation in oxygen minimum zones

Samantha G. Fortin, Xin Sun, Amal Jayakumar, Bess B. Ward

This file includes:
Supplemental Methods
Supplemental Discussion 1-3
Supplemental Figures S1-S7

In additional excel file:
Supplemental Tables S1-S6

Supplemental Methods

Additional Metagenomic Samples: Incubation, Sampling, and Sample Processing

Two depths were sampled at each station representing the shallow chlorophyll maximum and the deep chlorophyll maximum using 30-L Niskin bottles on a Seabird CTD rosette system before dawn. The Niskin bottles were plumbed with CO_2 (in the headspace, not sparging the water) while water was being transferred to the incubation bottles in order to minimize air contamination. Water was transferred directly to 4-L clear polycarbonate bottles wrapped in black plastic, filled to overflowing, and capped without bubbles or a headspace. Samples (TF) were incubated until late afternoon (Table S1) wrapped in opaque plastic in deck incubators at about 0.1% of surface light intensity and at surface seawater temperature of 27^{o}C, then filtered onto 0.22µm Sterivex capsules, frozen in liquid nitrogen, and stored at -80^{o}C until extraction using the All-Prep DNA/RNA Mini Kit. The quality of extracted DNA was verified by the 2100 Bioanalyzer System (Agilent, Santa Clara, CA). Randomly amplified DNA fragments were pair-end sequenced with Illumina HiSeq (Illumina, San Diego, CA) (180nt paired end). Quality check, random amplification, and sequencing were conducted by the Genomics Core Facility of Lewis-Sigler Institute for Integrative Genomics at Princeton University.

Primer Design and Development

The beta subunit of the nitrite oxidoreductase gene (*nxrB*), the gene commonly used for NOB phylogeny and identification [1], was identified in the NOB MAGs and in contigs from a subset of the ETNP samples using blast+ [2] and HMMER [3] with search templates based on previously identified *nxrB* gene sequences [4] and the *nxrB* model from the KBase HMMs of Environmental Bioelement application [5]. The resulting sequences were confirmed as *nxrB* by comparing to the NCBI GenBank database. An alignment was made of confirmed *nxrB* genes

using MEGA v11 [6] and used to search *in silico* for previously published *nxrB* primer sequences. Sequences matching existing primers were only found in a few OMZ *nxrB* sequences, therefore new primers were developed to target Nitrospinae *nxrB* genes from OMZs: nxrBomz1F (5' GAGTAYATGTGGTGGAAYAAYGT) and nxrBomz1R (5' CRTCCTCYTGGCGYTTGTA). The new primer set was checked for specificity using a blastn search against the NCBI GenBank database and was further confirmed by gel electrophoresis and the sequencing of clonally amplified fragments.

PCR Conditions, Creation of Standard, and Cloning

PCR conditions for amplification with primers nxrBomz1F and nxrBomz1R: 5μL of GoTaq buffer, 0.125μL of GoTaq, 0.5μL of dNTPs, 1μL of each primer (10pmol/μL), and 2μL of DNA, with the rest of the 25μL reaction consisting of water. The PCR program was: 95°C for 3min followed by 35 cycles of 95°C for 30s, 50°C for 40s, and 72°C for 1min, with a final elongation step of 72°C for 7min. Triplicate reactions were combined and purified using the Qiagen QIAQuick Gel Extraction kit and manufacturer protocols.

qPCR Optimization

The new primer set was used to amplify *nxrB* genes from a separate (not metagenomically sequenced) ETNP OMZ sample from 70m depth. The purified gene product from triplicate reactions was then inserted into a pGEM-T Easy Vector (Promega) and cloned into *E. coli* cells using established protocols. Cloned inserts were sequenced and confirmed to be *nxrB* with high identity to *nxrB* identified in the metagenomic samples. One cloned *nxrB* amplicon was used as a standard for qPCR.

The standard curve and 3 representative samples were used to optimize the qPCR reaction over a range of annealing temperatures (50 to 58°C), primer additions (0.5 to 2μL of

each primer), and template DNA additions (1 to 2μL). The optimized reaction included 6.25μL of QuantiTect master mix (Qiagen), 1μL of each primer (10pM; nxrBomz1F/R), and 1μL of template DNA or cDNA (ranging between 0.02 and 35ng/μL), with the rest of the 12μL reaction made up of water. The optimized qPCR protocol was as follows: 95ºC for 10 min, followed by 40 cycles of 95ºC for 30s, 52ºC for 40s, and 72ºC for 30s, followed by a melt curve to check for specificity of the reaction.

Based on the standard curve, created through a serial dilution of an *nxrB* cloned from an ETNP sample, the efficiency of the qPCR ranged between 46.6 and 54.7%. The efficiency of each individual reaction was also calculated based on the amplification curve [7] using the LinRegPCR program [8]. Using this method of efficiency calculation, *nxrB* DNA standards and samples had an efficiency of 86.9 and 85.2%, respectively. Due to the similar efficiency of standards and samples in individual reactions, the gene copy numbers determined from the standard curve are likely to accurately represent the true copy numbers in the environmental samples, despite the low standard curve-based efficiency. The primers used in the qPCR had several degeneracies, three each in the forward and reverse, in order to cover the wide range of *nxrB* found in the samples from three oxygen minimum zones which likely lowered the efficiency of the reaction.

Supplemental Discussion 1: Characteristics of OMZ stations

Samples were collected from the ETNP in two different years, and from the Arabian Sea (Figure S1). Each OMZ station had a sharp oxycline, an anoxic OMZ core (also referred to as the oxygen depleted zone, ODZ), and a primary and secondary nitrite maximum. Of the three 2018 ETNP stations, PS2 and PS3 were in the OMZ and had large secondary nitrite maxima, while PS1 bordered the OMZ and, though it had an ODZ, had only one nitrite maximum located in the

oxycline making it a non-OMZ station (Figure S6). Station PS3 was a coastal station and had a shallower oxycline depth than the two offshore stations. Two ETNP OMZ stations, PS6 and 14, were sampled in 2016. PS6 was a coastal station with a shallower oxycline depth than 14 (Figure S6). Only one station was sampled for metagenomic work in the Arabian Sea OMZ in 2007; it showed the characteristic oxygen depleted zone and larger secondary nitrite peak (Figure S6).

Supplemental Discussion 2: Quantifying NOB organisms

Relative abundance, even normalized by RPKM, can be influenced by a number of factors in OMZs as microbial diversity is influenced by depth and oxygen concentrations [9]. To account for any potential inaccuracies in the abundance of MAGs, the actual abundance of *nxrB* in both DNA and cDNA was determined using qPCR with primers that captured *nxrB* genes found in the ODZ NOB and the Clade 1a Nitrospinae. While *nxrB* is often found in two copies in *Nitrospina* genomes [10], the DNA based qPCR data still provides a more accurate count of how many *nxrB* genes, and therefore how many NOB, are present throughout the depth profile. The need for both relative and quantitative measurements can be seen in the conflicting observations of NOB3; the observed increase in RPKM of NOB3 at depth was not reflected in an increase in the DNA based abundance of *nxrB*. Therefore, it is likely the increase in NOB3 at depth indicates a shift in its importance in the entire community rather than an increase in the number of NOB3 cells at depth. Despite the discrepancy between NOB3 relative abundance and qPCR abundances, there is a significant positive linear relationship between the DNA based qPCR abundance of *nxrB* and the relative abundance of all NOB (i.e., ODZ NOB, SAG NOB, and

cultured NOB combined), showing that the metagenome and qPCR analyses support each other (Figure S7).

Supplemental Discussion 3: Phylogenetic relationship of expressed *nxrB* genes

The *nxrB* tree included: sequences cloned from the cDNA of the depth with the highest nitrite oxidation rate at stations ETNP PS1, ETNP PS2, ETNP PS3, and ETNP PS6, sequences obtained from ETNP PS2 130m and ETNP PS3 70m metagenomes, and sequences from OMZ MAGs, SAGs, and cultured organisms (Figure S2). Most branches in the tree were very short, making identification of NOB based on their *nxrB* genes difficult. However, one clade of the tree clearly grouped with *nxrB* genes from multiple NOB2 MAGs (yellow clade Figure S2) while a second grouped closely with one of the *nxrB* genes from NOB1 (green clade Figure S2). However, many of the sequences fell on a branch of the tree that included a *nxrB* gene from NOB1 and *nxrB* genes from SAG 1a (blue clade Figure S2). Two more large groups (Collapsed clades N86 and N42 Figure S2) contained *nxrB* genes only from clones and the metagenomes; this group is likely represented in the OMZ MAGs but, since not all MAGs contained *nxrB,* could not be identified at this time. While this suggests that *nxrB* may not be the ideal gene to separate the Clade 1a Nitrospinae at the species level, an endeavor that is likely complicated by NOB containing multiple copies of the *nxrB* gene, the cloned cDNA *nxrB* do indicate that the corresponding metagenomes are accurately representing the NOB community and its dominance by ODZ NOBs. Furthermore, since the cDNA was used for cloning, these NOB communities are actively producing RNA for *nxrB* at depths where nitrite oxidation is also present.

References

1. Pester M, Maixner F, Berry D, Rattei T, Koch H, Lücker S, et al. NxrB encoding the beta subunit of nitrite oxidoreductase as functional and phylogenetic marker for nitrite-oxidizing Nitrospira. *Environ Microbiol* 2014; **16**: 3055–3071. https://doi.org/10.1111/1462-2920.12300.
2. Camacho C, Coulouris G, Avagyan V, Ma N, Papadopoulos J, Bealer K, et al. BLAST+: Architecture and applications. *BMC Bioinformatics* 2009; **10**: 421. https://doi.org/10.1186/1471-2105-10-421.
3. Eddy SR. Accelerated profile HMM searches. *PLoS Comput Biol* 2011; **7**: e1002195. https://doi.org/10.1371/journal.pcbi.1002195.
4. Sun X, Kop LFM, Lau MCY, Frank J, Jayakumar A, Lücker S, et al. Uncultured Nitrospina-like species are major nitrite oxidizing bacteria in oxygen minimum zones. *ISME J* 2019; **13**: 2391–2402. https://doi.org/10.1038/s41396-019-0443-7.
5. Anantharaman K, Brown CT, Hug LA, Sharon I, Castelle CJ, Probst AJ, et al. Thousands of microbial genomes shed light on interconnected biogeochemical processes in an aquifer system. *Nat Commun* 2016; **7**: 13219. https://doi.org/10.1038/ncomms13219.
6. Tamura K, Peterson D, Peterson N, Stecher G, Nei M, Kumar S. MEGA5: Molecular evolutionary genetics analysis using maximum likelihood, evolutionary distance, and maximum parsimony methods. *Mol Biol Evol* 2011; **28**: 2731–2739. https://doi.org/10.1093/molbev/msr121.
7. Ruijter JM, Ramakers C, Hoogaars WMH, Karlen Y, Bakker O, van den hoff MJB, et al. Amplification efficiency: Linking baseline and bias in the analysis of quantitative PCR data. *Nucleic Acids Res* 2009; **37**: e45. https://doi.org/10.1093/nar/gkp045.
8. Untergasser A, Ruijter JM, Benes V, van den Hoff MJB. Web-based LinRegPCR: application for the visualization and analysis of (RT)-qPCR amplification and melting data. *BMC Bioinformatics* 2021; **22**: 398. https://doi.org/10.1186/s12859-021-04306-1.
9. Ganesh S, Parris DJ, Delong EF, Stewart FJ. Metagenomic analysis of size-fractionated picoplankton in a marine oxygen minimum zone. *ISME J* 2014; **8**: 187–211. https://doi.org/10.1038/ismej.2013.144.
10. Lücker S, Nowka B, Rattei T, Spieck E, Daims H. The genome of Nitrospina gracilis illuminates the metabolism and evolution of the major marine nitrite oxidizer. *Front Microbiol* 2013; **4**: 00027. https://doi.org/10.3389/fmicb.2013.00027.

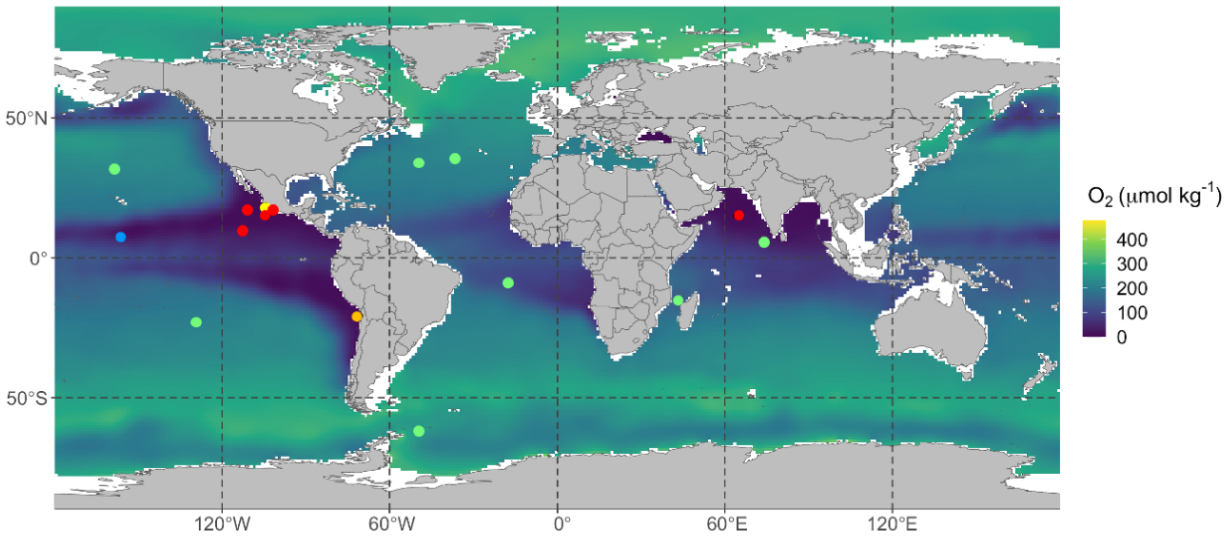

Figure S1. A map of all locations with metagenomic samples used in this study overlying the annual mean O_2 concentration (from 1955 to 2017, World Ocean Atlas) at 200m below the surface. Red indicates OMZ samples from this study where new NOB MAGs originated. The remaining colors indicate the location of previously published metagenome samples: oxygenated open ocean (green; Tara Oceans), ETSP 2013 OMZ (orange), ETNP 2013 OMZ (yellow), and ETNP 2011 bordering the OMZ (blue). More details on the metagenomic samples can be found in Tables S1 and S4.

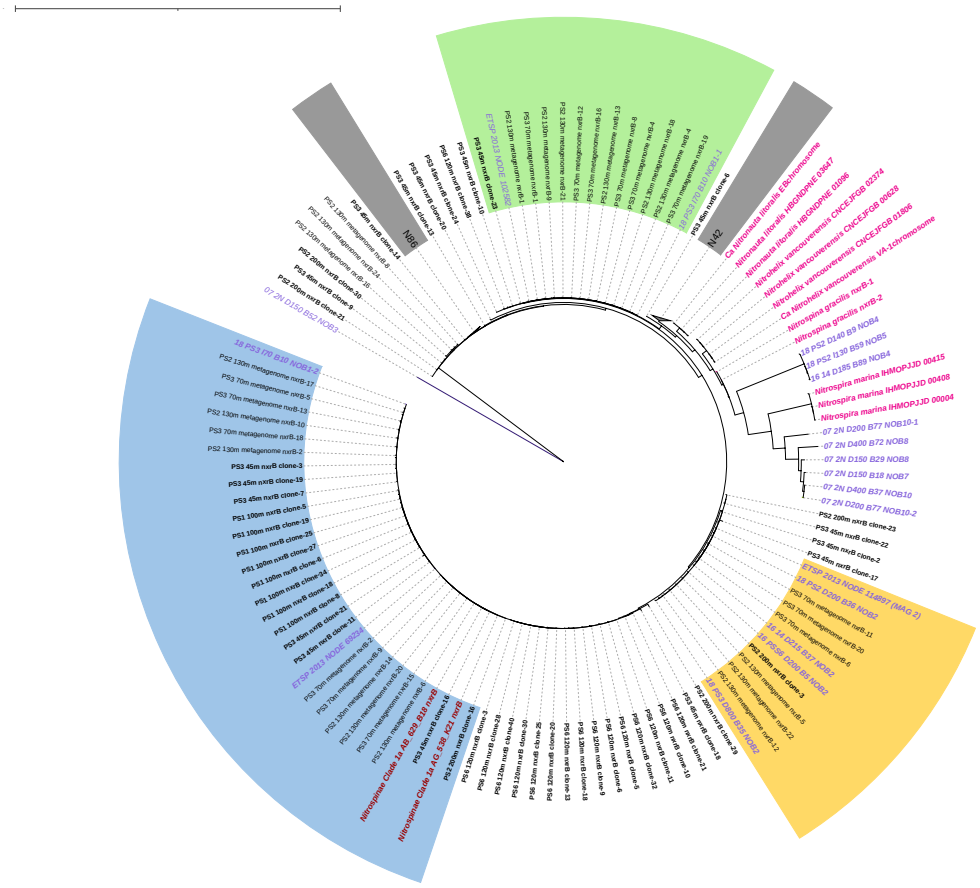

Figure S2. Phylogenetic tree of *nxrB* genes from NOB ODZ MAGs (purple), cultured NOB genomes (pink), Nitrospinae Clade 1a SAGs (red), cDNA clones (bold), and metagenome sequences. Blue clade represents sequences resembling NOB1 and SAG 1a, green clade represents sequences resembling NOB1, and yellow clade represents sequences resembling NOB2. Collapsed clade N86 includes *nxrB* sequences from: PS1 100m cDNA clones (n=38), PS6 120m cDNA clones (24), PS2 200m cDNA clones (7), PS2 130m metagenome (6), PS3 70m metagenome (6), and PS3 45m cDNA clones (4). Collapsed clade N42 includes *nxrB* sequences from: PS2 200m cDNA clones (17) and PS3 45m cDNA clones (3). Scale bar represents a branch length of 10.

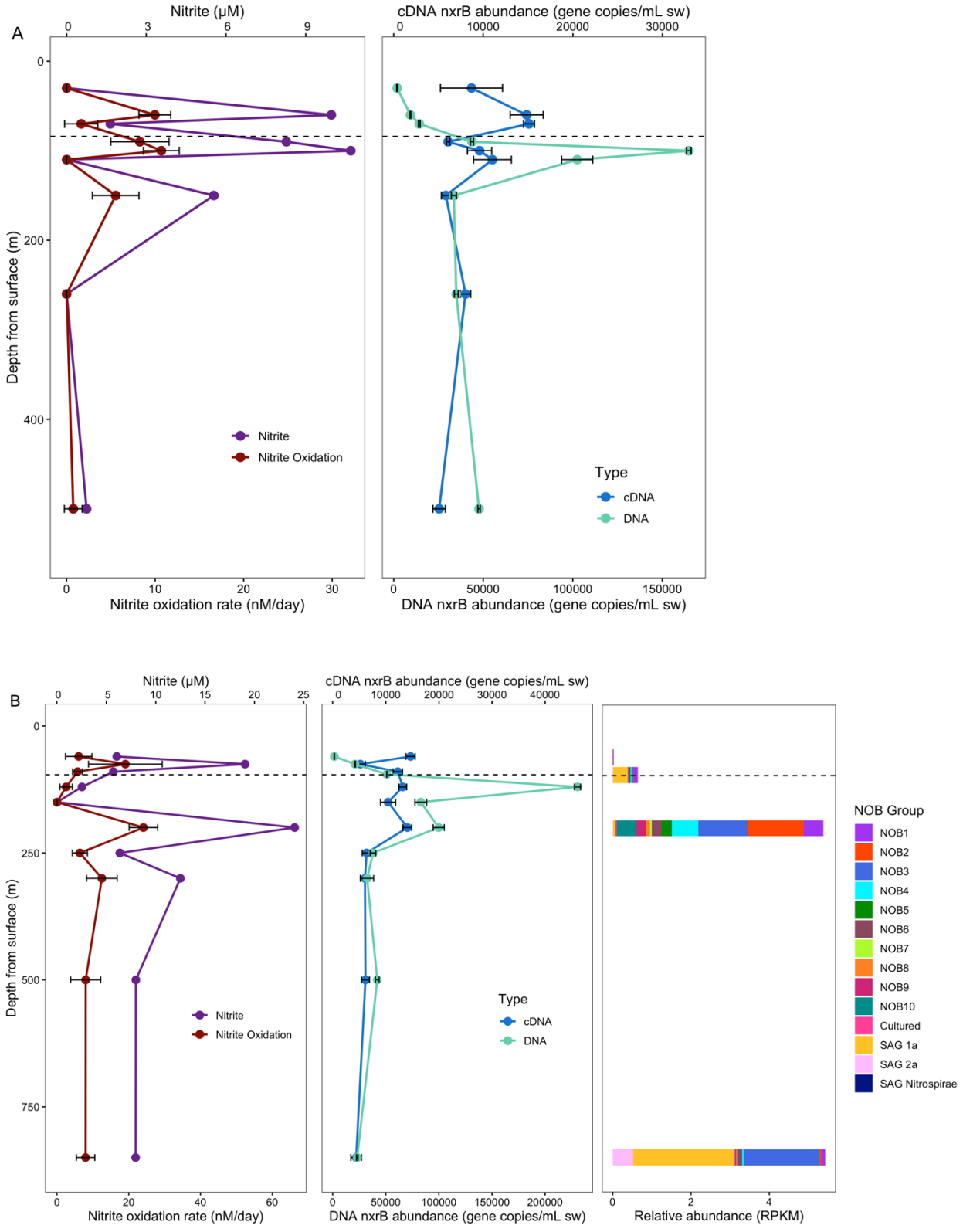
A
Nitrite (μM)
cDNA nxrB abundance (gene copies/mL sw)
Depth from surface (m)
Nitrite
Nitrite Oxidation
Type
cDNA
DNA
Nitrite oxidation rate (nM/day)
DNA nxrB abundance (gene copies/mL sw)
B
Relative abundance (RPKM)
NOB Group
NOB1
NOB2
NOB3
NOB4
NOB5
NOB6
NOB7
NOB8
NOB9
NOB10
Cultured
SAG 1a
SAG 2a
SAG Nitrospirae

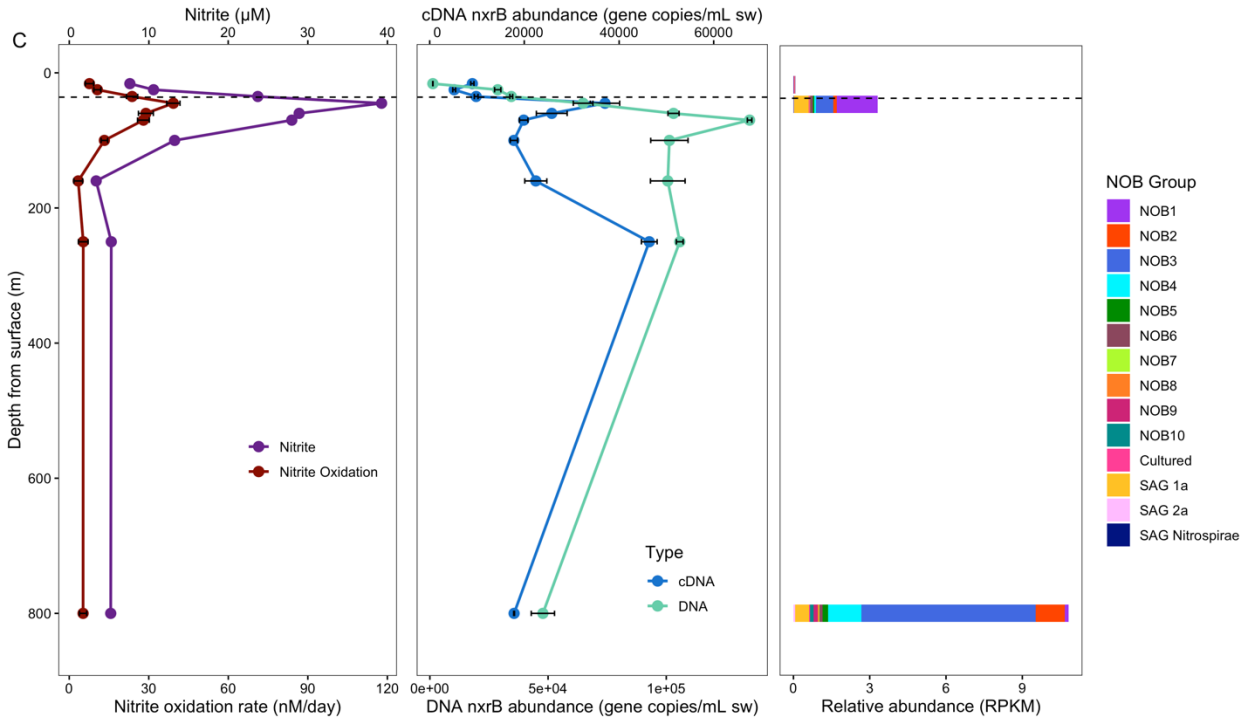
C
Nitrite (μM)
cDNA nxrB abundance (gene copies/mL sw)
Depth from surface (m)
Nitrite
Nitrite Oxidation
Type
cDNA
DNA
Nitrite oxidation rate (nM/day)
DNA nxrB abundance (gene copies/mL sw)
Relative abundance (RPKM)
NOB Group
NOB1
NOB2
NOB3
NOB4
NOB5
NOB6
NOB7
NOB8
NOB9
NOB10
Cultured
SAG 1a
SAG 2a
SAG Nitrospirae

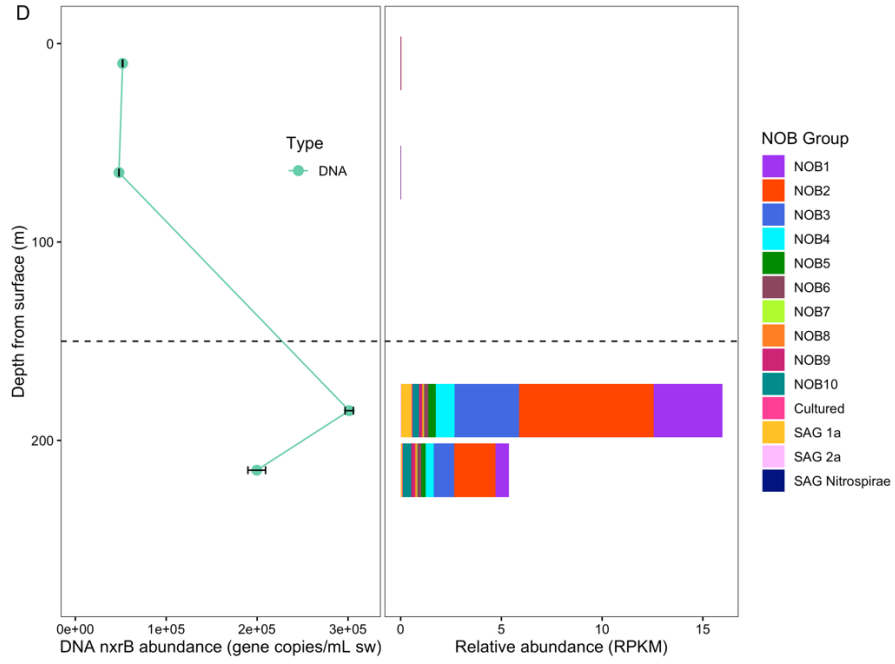
D
Depth from surface (m)
Type
DNA
DNA nxrB abundance (gene copies/mL sw)
Relative abundance (RPKM)
NOB Group
NOB1
NOB2
NOB3
NOB4
NOB5
NOB6
NOB7
NOB8
NOB9
NOB10
Cultured
SAG 1a
SAG 2a
SAG Nitrospirae

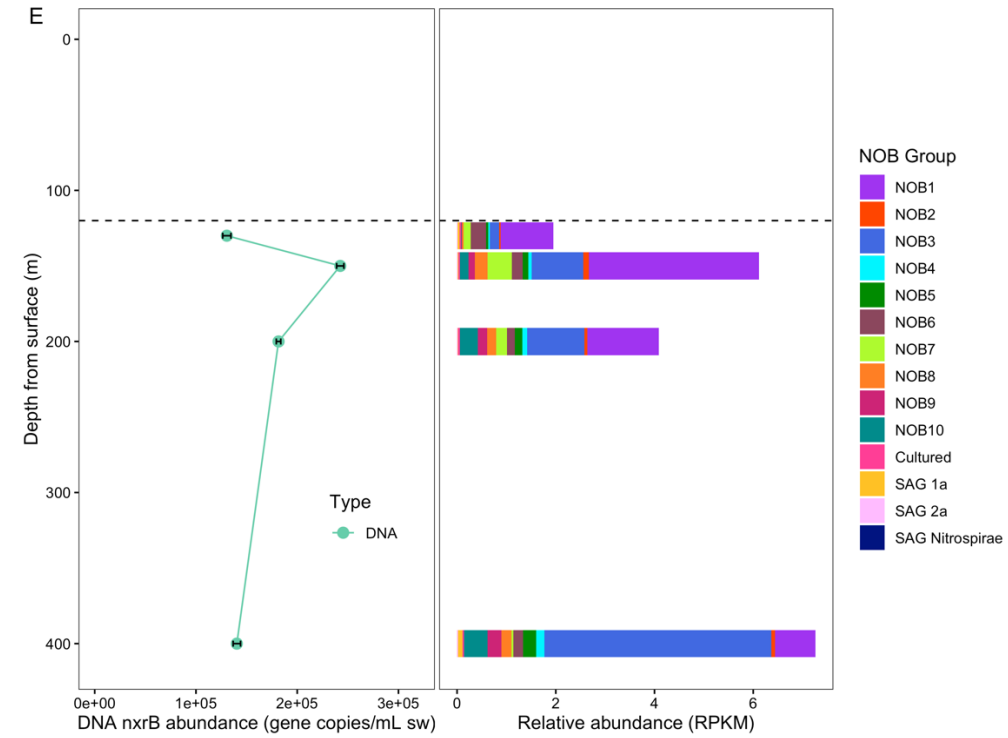

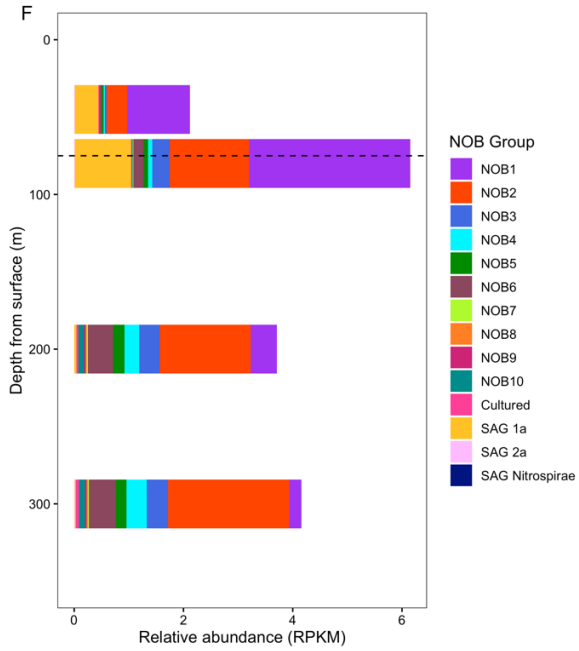

Figure S3. The nitrite oxidation rate (nM/day), DNA and cDNA based *nxrB* gene abundance (gene copies/mL seawater), and the abundance (RPKM) of NOB groups in station **(A)** ETNP PS1, **(B)** ETNP PS2, **(C)** ETNP PS3, **(D)** ETNP 14, **(E)** Arabian Sea, **(F)** ETSP 2013, plotted against the depth (m) below the surface. Error bars represent standard error; nitrite oxidation error bars are from biological replicates, *nxrB* abundance error bars are from technical replicates.

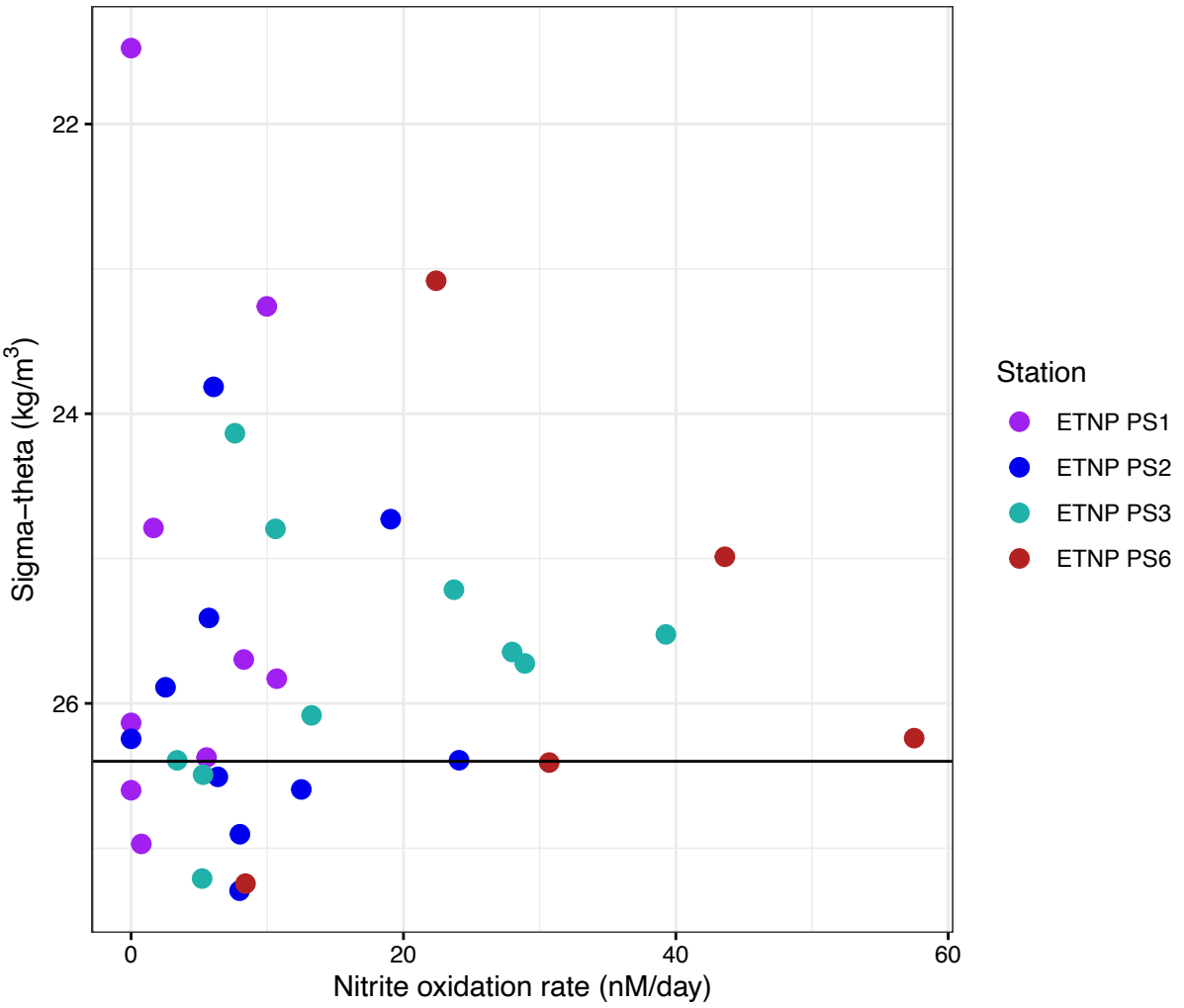

Figure S4. A scatter plot of density (σt, kg/m^3) versus nitrite oxidation rates (nM/day) at stations ETNP PS1, PS2, PS3, and PS6. The black line represents a σt of 26.4.

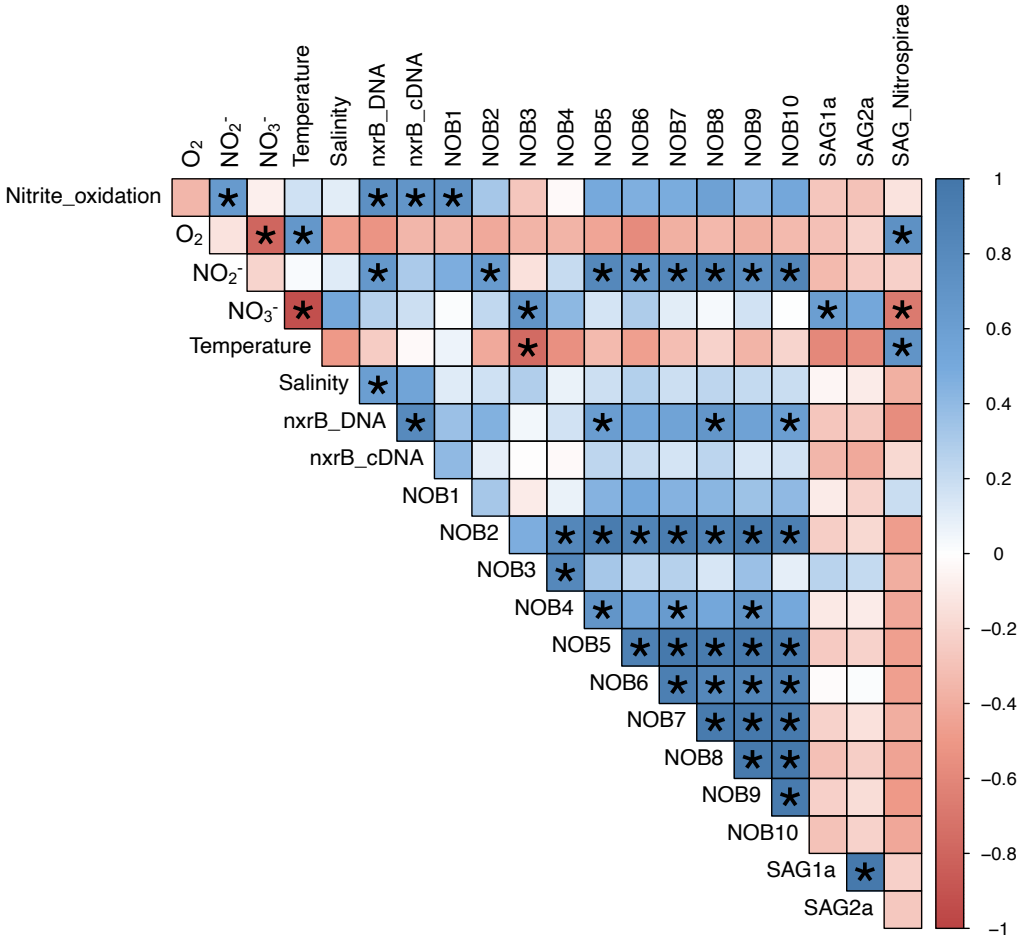

Figure S5. Pearson correlations comparing environmental variables and the RPKM of NOB groups from Stations ETNP PS2, ETNP PS3, and ETNP PS6. A star (*) indicates a significant correlation ($p<0.05$). Colors represent Pearson correlation value. Environmental variables include: nitrite oxidation rates (Nitrite_oxidation), concentration of O_2, NO_2, NO_3, seawater temperature and salinity, the *nxrB* abundance based on DNA and cDNA, and the relative abundance (RPKM) of the each ODZ NOB group and each NOB SAG; cultured organisms were not included because most had zero relative abundance across all the included samples. This figure shows the same data as Figure 3 for the first 8 rows.

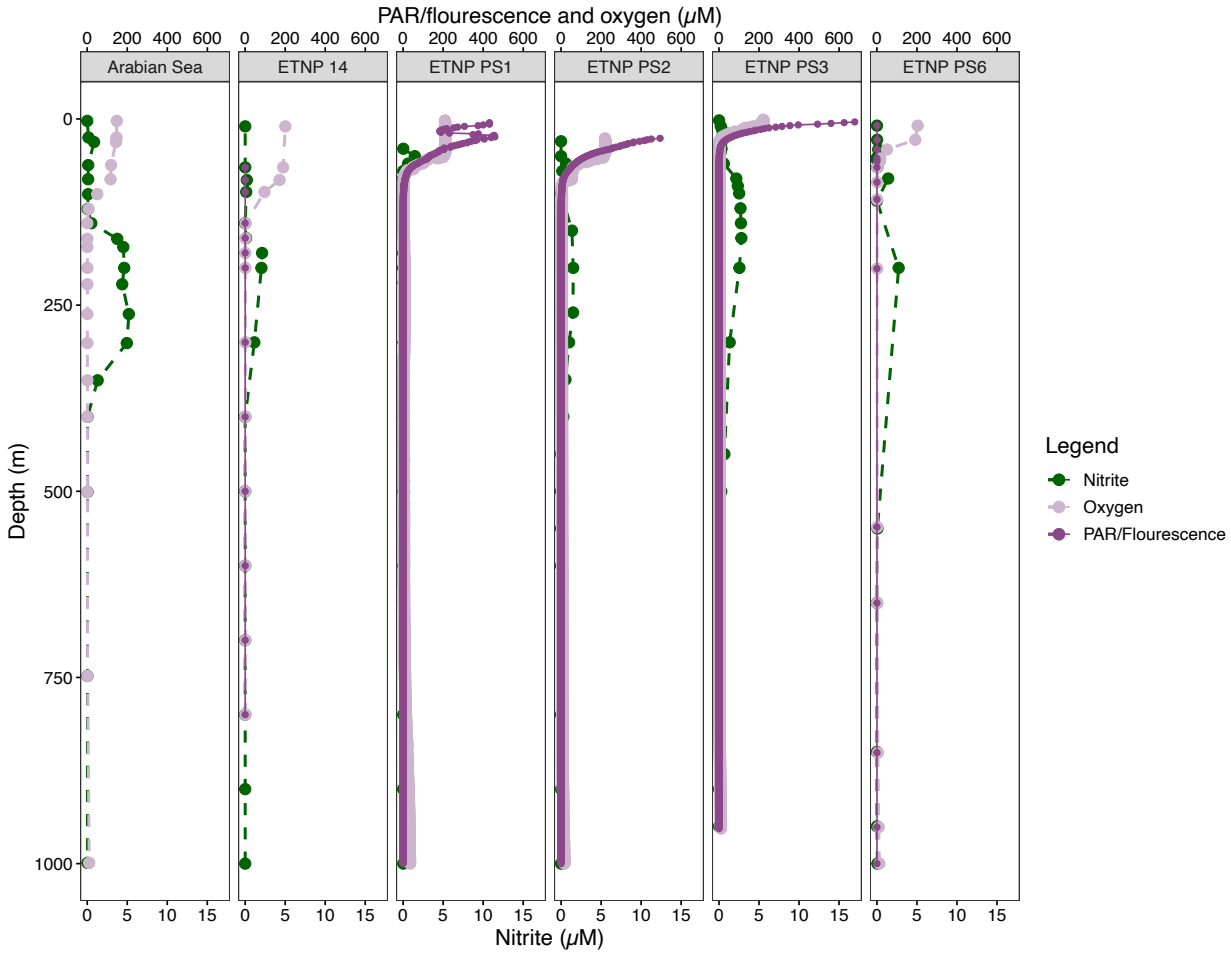

Figure S6. Depth profiles of OMZ stations representing the concentration of nitrite (green), oxygen (pink), and PAR or fluorescence (purple). ETNP PS1, PS2, and PS3 had PAR measurements (microEinsteins/m^2); ETNP 14 and ETNP PS6 had fluorescence (μg/L) measurements; Arabian Sea had neither PAR or fluorescence measurements.

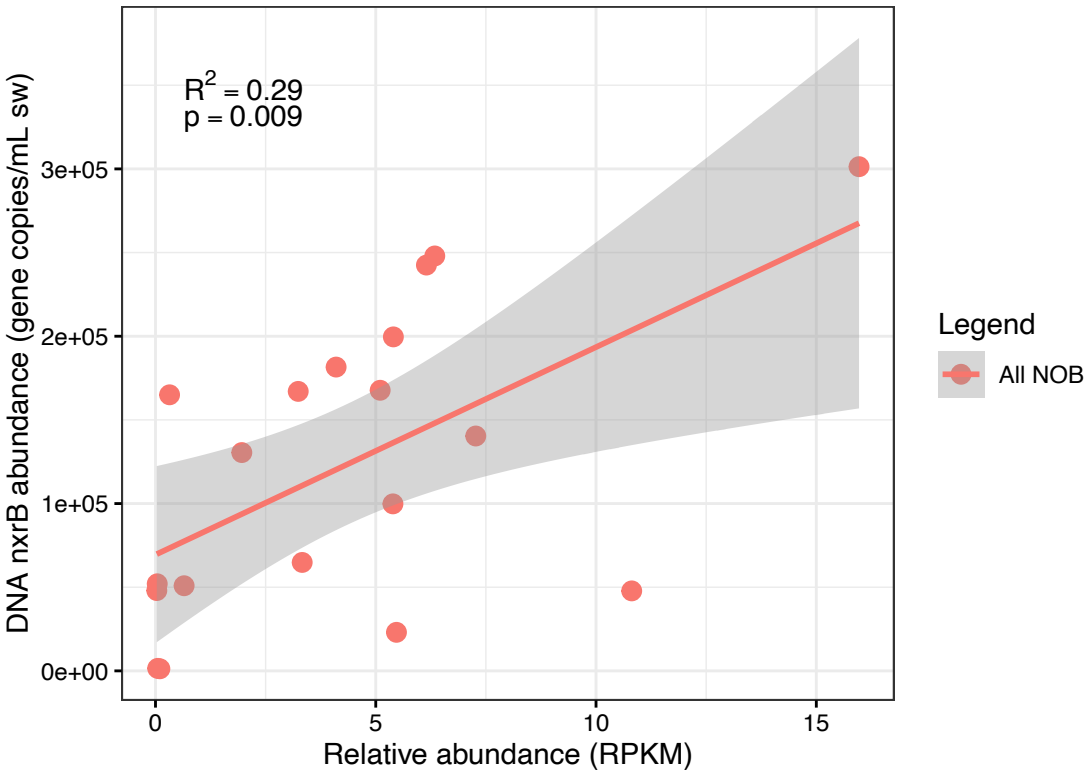

Figure S7. DNA based *nxrB* abundance (gene copies/mL seawater) determined by qPCR compared to relative abundance (RPKM) of all NOB including ODZ NOB, SAG NOB, and cultured NOB. Line represents the linear regression (obtained using ggplot2 lm setting in geom_smooth function) with the adjusted R^2 and p-value of the linear regression reported in the top left corner.